Uspostava tumorske linije debelog crijeva s mutacijom u genu B7H3 i njena funkcionalna analiza

Južnić, Lea

Master's thesis / Diplomski rad

2017

University of Zagreb

Faculty of Science

Department of Biology

Lea Južnić

Generation of colorectal cancer cell line with mutation in B7H3 gene and its functional analysis

Uspostava tumorske linije debelog crijeva s mutacijom u genu B7H3 i njena funkcionalna analiza

Graduation Thesis

Zagreb, 2017.

This thesis was conducted in the laboratory of Prof. Dr. med. Sebastian Zeissig at the Center for Regenerative Therapies Dresden, Cluster of Excellence, TU Dresden, under supervision of Prof. Dr. med Sebastian Zeissig and co-supervision of Dr. Maja Matulić, Assoc. Prof. The thesis was submitted for evaluation to the Department of Biology, Faculty of Science, University of Zagreb in order to obtain the title of Master of Molecular Biology (mag.biol.mol.).

Acknowledgements

Sveučilište u Zagrebu

Prirodoslovno-matematički fakultet

Biološki odsjek   Diplomski rad

USPOSTAVA TUMORSKE LINIJE DEBELOG CRIJEVA S MUTACIJOM U GENU B7-H3 I NJENA FUNKCIONALNA ANALIZA

Lea Južnić

Rooseveltov trg 6, 10000 Zagreb, Hrvatska

Tumori uspostavljaju različite mehanizme kako bi se zaštitili od protu-tumorskog odgovora imunološkog sustava. Ljudski imunološki sustav stoga sadrži niz različitih regulatornih molekula, koje mogu stimulirati ili inhibirati imunološke reakcije. Pri tom, receptori i ligandi iz CD28 i B7 obitelji imaju središnju ulogu u posredovanju interakcija između tumorskih i imunoloških stanica. B7 homolog 3 (B7-H3, *Cd276*) opisan je kao član obitelji B7 koji je aberantno eksprimiran u različitim tumorima, uključujući rak debelog crijeva (CRC). Prethodna istraživanja pokazala su kontradiktorne uloge B7-H3 unutar imunološkog sustava, upućujući na imunosupresivno i imunostimuliratorno djelovanje. Dodatno, nekoliko je studija pokazalo da je B7-H3 uključen u intrinzičnu regulaciju razvoja i progresije tumora, poput apoptoze, proliferacije, migracije, invazije i metastaza. Stoga, kako bi se razjasnila potencijalna uloga B7-H3 u CRC-u, ovaj je rad imao za cilj uspostaviti tumorsku liniju raka debelog crijeva bez ekspresije B7-H3 uz pomoć CRISPR/Cas9 sustava, te istražiti potencijalne autonomne uloge B7-H3 molekule neovisno o imunološkom sustavu. Analiza pomoću metoda qRT-PCR-a, Western blota i imunofluorescencije pokazala je nedostatak B7-H3 nakon što su mutacije uvedene. Nadalje, apoptoza i proliferacija nisu promijenjene u stanicama koje su deficijentne za B7-H3. Prema tome, rezultati ovog rada upućuju na to da B7-H3 ne regulira staničnu smrt i proliferaciju tumora na staničnoj razini, već potencijalno posredno djeluje putem kontrole aktivacije imunološkog odgovora.

University of Zagreb

Faculty of Science

Department of Biology   Graduation Thesis

GENERATION OF COLORECTAL CANCER CELL LINE WITH MUTATION IN B7-H3 GENE AND ITS FUNCTIONAL ANALYSIS

Lea Južnić

Rooseveltov trg 6, 10000 Zagreb, Croatia

Tumors establish a variety of different mechanisms to protect themselves from immune-mediated recognition and rejection. The human immune system is orchestrated by a variety of different regulatory molecules, which can either stimulate or inhibit immune cell responses. Receptors and ligands of the CD28 and B7 family have a central role in regulating the interaction between tumor and immune cells. The B7 homolog 3 (B7-H3, *Cd276*) has been described as a member of the B7 family which is aberrantly expressed in various tumors, including colorectal cancer (CRC) where its expression has also been shown to correlate with poor prognosis. Previous studies showed contradictory roles of B7-H3 within the immune system, demonstrating both immunosuppressive and immunostimulatory actions. In addition, it was suggested that B7-H3 may regulate tumor apoptosis, proliferation, migration, invasion and metastasis in a cell-autonomous manner. To address the question of potential cell-autonomous actions of B7-H3 in CRC, this work aimed at the generation of a CRC cell line with mutated B7-H3 using the CRISPR/Cas9 system and the investigation of potential cell-intrinsic functions of B7-H3. Analysis via qRT-PCR, Western blot and immunofluorescence methods showed a lack of B7-H3 after mutations were introduced in the *Cd276* gene coding for B7-H3. Furthermore, apoptosis and proliferation were unaltered in cells deficient for B7-H3. Therefore, the results of this work suggest that B7-H3 does not regulate CRC cell death and proliferation in a cell-intrinsic manner but rather acts indirectly through the control of immune cell activation.

TABLE OF CONTENTS

LIST OF ABBREVIATIONS AND ACRONYMS

7-AAD	7-aminoactinomycin D
Ann	Annexin V
APC	antigen-presenting cell
APC	adenomatous polyposis coli
B7-H3, *Cd276*	B7 homolog 3
BRAF	v-Raf murine sarcoma viral oncogene homolog B
BrDU	bromodeoxyuridine
CRC	colorectal cancer
CRISPR	clustered regularly interspaced short palindromic repeats
CTL	cytotoxic T lymphocytes
CTLA4	cytotoxic T lymphocyte associated antigen 4
D-PBS	Dulbecco's phosphate-buffered saline
DAPI	4',6-diamidino-2-phenylindole
DMEM	Dulbecco's Modified Eagle Medium
DMSO	dimethyl sufoxide
DTT	dithiothreitol
FBS	fetal bovine serum
GM-CSF	granulocyte-macrophage colony stimulating factor
IFN-γ	interferon gamma
KRAS	Kirsten rat sarcoma viral oncogene homolog
MHC	major histocompatibility complex
MLH1	MutL homolog 1
MMP	matrix-metalloproteinase
MTT	3-(4,5-dimethylthiazol-2-yl)-2,5-diphenyltetrazolium bromide
NK	natural killer
PCR	polymerase chain reaction

PD-L1	programmed cell death ligand 1
PMA	phorbol 12-myristate 13-acetate
PNGase F	Protein-N-Glycosidase F
PVDF	polyvinylidene difluoride
qRT-PCR	quantitative real-time polymerase chain reaction
RIPA	radioimmunoprecipitation assay
s.e.m.	standard error of the mean
SDS-PAGE	sodium dodecyl sulfate polyacrylamide gel electrophoresis
TAM	Tumor-associated macrophage
TBS-T	Tris-buffered saline with Tween 50
TCR	T cell receptor
TP53	Tumor protein p53
TREML2, TLT-2	triggering receptor expressed on myeloid cell-like transcript 2

1   INTRODUCTION

1.1   Colorectal cancer

Colorectal cancer (CRC) is the third most common malignancy and the fourth leading cause of death in the global human population, accounting for about 1.4 million new cases and almost 700 000 deaths in 2012 worldwide (Ferlay *et al*, 2015). These numbers are expected to annually increase to more than 2.2 million new cases and 1.1 million cancer deaths by 2030 worldwide (globocan.iarc.fr 2017).

Colorectal cancer is a result of multiple risk factors that co-occur and interact. They include sociodemographic factors, such as old age and male sex (Brenner *et al*, 2014), family history of CRC (Taylor *et al*, 2010), predisposing diseases like inflammatory bowel disease (Jess *et al*, 2012), obesity (Ma *et al*, 2013) or diabetes (Jiang *et al*, 2011), lifestyle and environmental factors such as smoking (Liang *et al*, 2009), excessive alcohol consumption (Fedirko *et al*, 2011) and high consumption of red and processed meat (Chan *et al*, 2011) or the intestinal microbiota (Lucas *et al*, 2017). Within the microbiota, colonization with *Bacteroides fragilis* or *Fusobacterium* spp has also been implicated in CRC growth (Brenner *et al*, 2014). These risk factors can promote a sporadic onset of CRC which is the case for about 90% of all CRC cases (Lucas *et al*, 2017). As previously mentioned, also familial inheritance for CRC can occur, which accounts for approximately 10% of all cases. Depending on inherited genetic alterations involved, it is possible to distinguish two main forms of hereditary CRC – Lynch syndrome (hereditary non-polyposis colorectal cancer; mutations in DNA mismatch repair) and familial adenomatous polyposis (germline mutations in the *APC* gene) (Lucas *et al*, 2017).

1.1.1   Molecular pathogenesis

All of the above mentioned causes of CRC can lead to genetic instability, reduced DNA integrity and subsequently to the loss of DNA stability which allows the accumulation of mutations (Terzic *et al*, 2010). Somatic mutations in defined genes are required to initiate and promote CRC development along the adenoma-carcinoma sequence (Fig 1.). Among the earliest events occurring in CRC are mutations in the tumor suppressor gene adenomatous polyposis coli (*APC*). Progression to malignancy is further promoted by activating mutations in the Kirsten rat sarcoma viral oncogene homolog (*KRAS*) and inactivating mutation of tumor protein p53 (*TP53*), a tumor suppressor gene. Additionally, mutations in the v-Raf murine sarcoma viral oncogene homolog B (*BRAF*) with CpG island methylator phenotype, as well as

MutL homolog 1 (*MLH1*) gene promoter methylation which leads to high levels of microsatellite instability, are also causes for CRC development (Brenner *et al*, 2014). Therefore, loss of control of cell proliferation, unlimited cell growth and hence tumor development are orchestrated by mutations in a variety of genes which are introduced over time.

CRC development begins with the formation of a hyper-proliferative intestinal epithelium, which thereby loses its cellular organization and consequently structure and ultimately leads to the formation of benign polyps or adenomas (Fig 1.). Some of these adenomas develop into adenocarcinoma while accumulating more genetic mutations, which can take up to 10 years. Later on, cancerous cells may invade surrounding tissue even further, reaching lymph nodes or blood vessels and leading to metastasis to the liver and/or the lung (Davies *et al*, 2005).
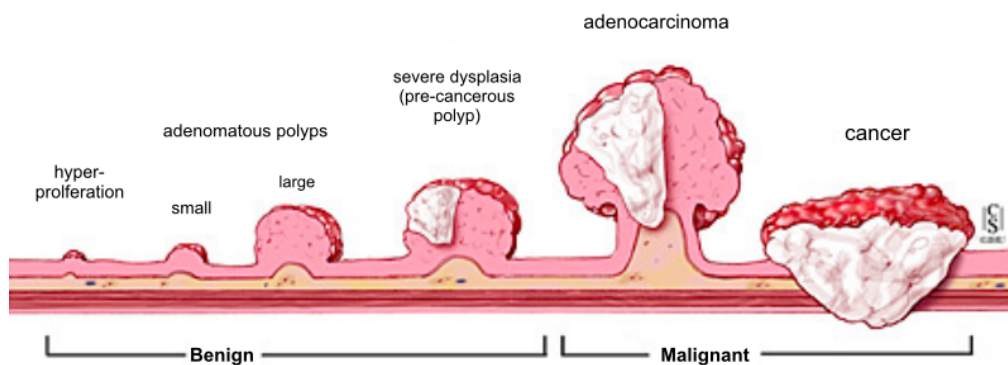
Figure 1. Adenoma-carcinoma sequence. Somatic mutations lead from hyper-proliferative epithelium to adenomas, adenocarcinomas and ultimately cancer (hopkinscoloncancer.org 2017)

1.2   Immune system

Once a tumor is established, processes to evade recognition by the host immune system are activated. The immune system is a host defense system which uses a complex array of protective mechanisms in order to control and eliminate pathogenic organisms, infectious agents, toxins or cancer cells. The immune system is conceptually divided into two parts – the innate immune system and the adaptive immune system (humoral or cell-mediated), both of which have characteristic features.

Innate immunity involves rapid immune responses after a pathogen is encountered and therefore leads the host's initial response. In the intestine, it comprises various physical barriers (epithelial or mucus layers), soluble proteins and biomolecules (cytokines, chemokines,

complement proteins) as well as membrane-bound or cytoplasmic receptors which bind molecular patterns expressed on surfaces of microbes. Cells included in innate immune response are neutrophils, basophils, eosinophils, dendritic cells, natural killer (NK) cells and monocyte-derived macrophages (Chaplin, 2010).

In addition, adaptive immunity leads to a slower, but more targeted response. It depends on antigens presented by antigen presenting cells (APCs), which are recognized by B and T lymphocytes in the context of major histocompatibility (MHC) molecules (Pecorino, 2012). MHC molecules are cell surface glycoproteins that bind fragments of proteins that have either been synthesized within the cell (MHC class I, MHCI) or ingested by the cell and proteolytically processed (MHC class II, MHCII). These mentioned lymphocytes express respective antigen-specific receptors that are encoded by genes assembled through somatic rearrangement of germ-line gene elements. In this way, the immune system creates a great variety of antigen receptors, each with potentially unique specificity for a different antigen (Chaplin, 2010).

However, T and B lymphocytes respond differently upon antigen recognition. Main functions of B cells are to synthesize and secrete antibodies, therefore contributing to humoral immunity. In contrast, T cells, specifically $CD8^+$ cytotoxic T cells (CTLs) and $CD4^+$ T helper cells (Th1, Th2, Th17, regulatory T cells), are responsible for cell-mediated immunity and mostly eliminate virally infected cells and tumor cells. They are activated through a broad spectrum of transmembrane heterodimeric proteins called T cell receptors (TCRs). Additionally, TCRs require accessory chains (CD3) which allow signal transduction after antigen recognition, leading to the activation of T cells. Activated T cells release perforins or granzymes, and express ligands for death receptors on the target cells. Because of high specificity and strict control of T cell activation and host-pathogen discrimination, cytotoxic T cell responses are considered as one of the most important anti-tumor defenses of the body (Pecorino, 2012). On the other hand, as inflammation is one of the main drivers of cancer development, active T cells can also exert protumorigenic functions by establishing and maintaining inflammatory tumor environment. Therefore, the immune system is an important regulator of tumor growth.

1.2.1 Immunosurveillance, immunoediting and immune escape

When the immune system recognizes and eliminates primary developing tumors, immunosurveillance takes place. It is expected that the immune system can recognize tumor-specific antigens (molecules that are unique to cancer cells) or tumor-associated antigens

(molecules that are differently expressed in cancer and healthy cells) and start to eliminate the tumor cells (Pecorino, 2012). It has been shown that components of both the adaptive and the innate immune system are involved in immunosurveillance (Marcus *et al*, 2014). Means of action depend on tumor's origin, mechanism of transformation, anatomic localization and mechanism of immunological recognition (Dunn *et al*, 2004).

Tumors can escape or limit immunosurveillance and even shift the immune response to a tumor-promoting role. This concept was termed immunoediting due to the fact that cancer cells are constantly able to modulate and edit the host's anti-tumor immune response (Pecorino, 2012). This is facilitated by a specific tumor microenvironment which is characterized by a chronic intrinsic inflammatory response that leads to the recruitment of various innate and adaptive immune cells (Grivennikov *et al*, 2010). Their abundance and activation state as well as the expression of various immune mediators and modulators dictate whether the immune cells will drive tumor-promoting inflammation or anti-tumor immunity.

The immune cells most frequently found within the tumor microenvironment are tumor associated macrophages (TAMs) and T lymphocytes (Grivennikov *et al*, 2010). TAMs usually promote tumor growth and are considered important for angiogenesis, invasion and metastasis (Condeelis i Pollard, 2006). On the other hand, T cells can exert both tumor-suppressive and tumor–promoting effects. The presence of activated CTLs or Th1 cells correlates with better survival in some cancers such as colon cancer or melanoma. However, many of the same T cell subsets are also involved in tumor promotion, progression or metastasis in other types of cancers. (Grivennikov *et al*, 2010). On the other hand, it is known that Th17 cells and its secreted interleukins have a prominent role in early stages of CRC development as shown in CRC patients with elevated levels of IL-17A which had a drastic reduction in survival rates (Formica *et al*, 2014; De Simone *et al*, 2013; Tosolini *et al*, 2011). Therefore, modulating T cell activation within the tumor microenvironment has been rapidly studied in the past years and shall further be explained.

1.2.2   The role of co-stimulatory and co-inhibitory molecules in T cell activation

In order to activate T cells, two stimuli are required. First, the before mentioned TCR/CD3 complex is able to interact with antigens only in the context of MHC molecules. However, this interaction provides only a partial signal for T cell activation. The second signal originates from interactions of the CD28 family of receptors on T cells with the B7 family of ligands on APCs (Fig. 2) (Chaplin, 2010; Ni i Dong, 2017). The second signal can be co-stimulatory or co-inhibitory, either promoting or inhibiting T cell activation. The absence of a co-stimulator, the first interaction leads to an anergic state of prolonged T cell non-responsiveness (Chaplin, 2010).
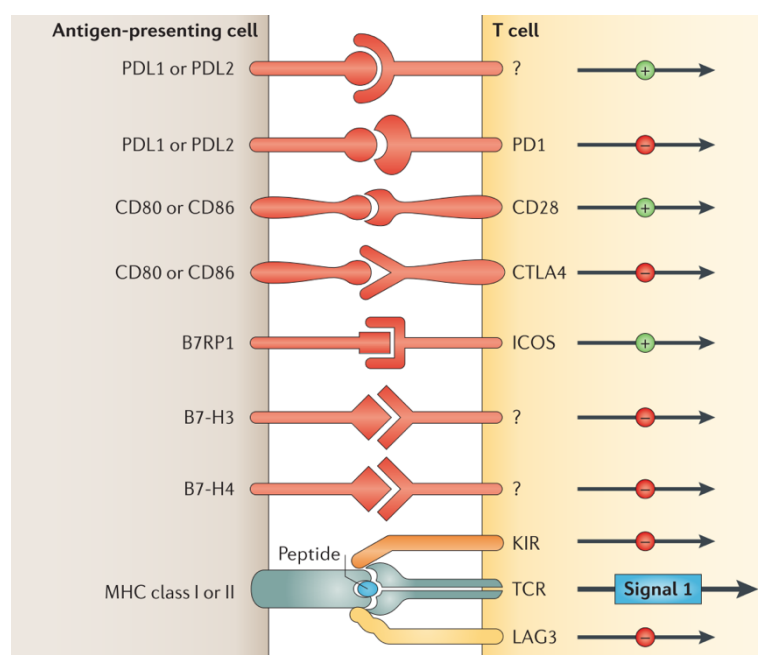
Figure 2. Overview of CD28/B7-family members on APCs and T cells. MHC class I or II interaction with TCR gives rise to the first signal for T cell activation. B7 ligands on APCs bind multiple receptors on T cells which can deliver co-stimulatory or co-inhibitory signals. For some of the newly identified B7 members, the respective receptor still remains unknown (Pardoll, 2012)

Many recent studies investigated properties of these co-stimulatory and co-inhibitory molecules, which are involved in the interaction between APCs and T cells (Figure 2). One example are ligands of the B7 family such as B7.1 (CD80) and B7.2 (CD86) which are expressed on APCs and interact with receptors on T cells such as CD28 or the cytotoxic T lymphocyte associated antigen 4 (CTLA4) to promote or inhibit T cell activation, respectively. As CD80 and CD86 are induced or up-regulated on stimulated APCs, they interact with CD28 receptors on T cells and enhance TCR-mediated signaling and promote T cell survival, leading to clonal expansion and differentiation of effector T cells (Lenschow *et al*, 1996). After T cell activation, CTLA4 is induced and CD80/CD86 binding leads to the down-regulation of T cell

proliferation (Suh *et al*, 2003). There are about 10 other B7 proteins which are structurally related to CD80 and CD86 and can be expressed in multiple organs with non-immune function, as well as on APCs. In this way, self-tolerance is maintained and tissues are protected from damage when the immune system is reacting to pathogenic infection. However, expression of both ligands or receptors might be dysregulated in tumors, which are therefore taking part in one of the additional mechanisms of immune escape. Generally, it is expected for inhibitory ligands or receptors which regulate T cell effector functions in tissues, to be overexpressed on tumor cells or non-transformed cells within tumor microenvironment (Pardoll, 2012). One important example of this case is programmed cell death ligand 1 (PD-L1), which was found to be expressed in many immune but also cancer cells and leads to the co-inhibition of T cell activation, and therefore impaired cytokine production as well as loss of cytotoxicity of activated T cells (Ni i Dong, 2017). Since this thesis focuses on the function of B7 homolog 3 (B7-H3), it shall further be explained in more detail.

1.3   B7 homolog 3

B7-H3 (CD276) is an immunoregulatory proteins of the B7 family that was discovered in 2001 (Chapoval *et al*, 2001). It is located on chromosome 15 in humans and chromosome 9 in mice. The gene, comprised of 10 exons, gives rise to a 316 amino acid long type I transmembrane glycoprotein belonging to the immunoglobulin superfamily with an expected molecular weight of 45-66 kDa. Due to exon duplication in humans it can be found in two isoforms depending on the number of pairs of V-like and C-like immunoglobulin domains – 4IgB7H3 or 2IgB7H3, while in mice only 2Ig forms are present (Fig. 3) (Janakiram *et al*, 2017).
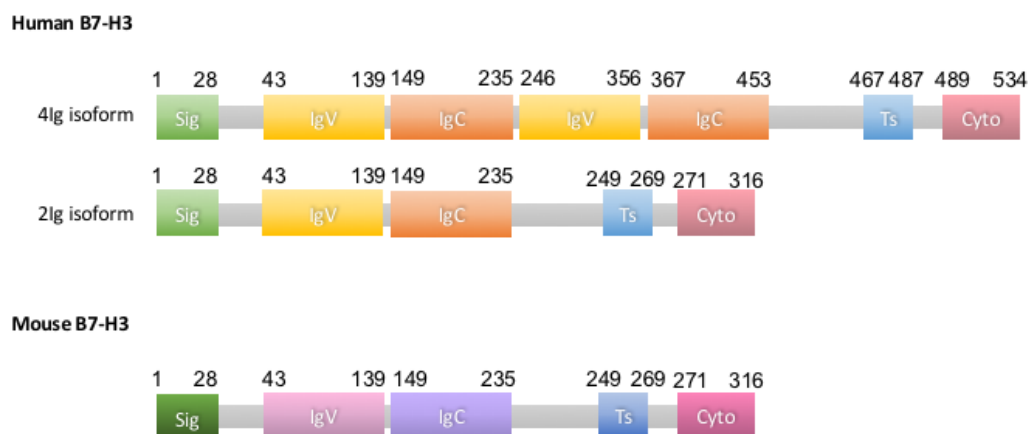
Figure 3. The structure of human and mouse B7-H3. Numbers on top represent amino acid numbers. Sig - signal peptide; IgV - V-like Ig; IgC - C-like Ig; Ts - transmembrane region; Cyto - cytoplasmic tail (adapted from Wang *et al*, 2014)

The interacting receptor on T cells still remains to be determined, as triggering receptor expressed on myeloid cell-like transcript 2 (TLT-2, TREML2) had been described as its costimulatory receptor in mice (Hashiguchi *et al*, 2008), but was not confirmed by other studies (Leitner *et al*, 2009).

B7-H3 is one the most evolutionary conserved B7 family member as it is universally expressed across various species from fish to mammals on mRNA-level (Sun *et al*, 2011). Furthermore, its mRNA is widely expressed in many tissues such as heart, prostate, testis, uterus, liver, pancreas, small intestine and colon (Chapoval *et al*, 2001). Low expression was also found in brain, skeletal muscle, kidney, lung and some lymphoid organs (Chapoval *et al*, 2001). Its expression by immune cells such as T cells and APCs (dendritic cells, macrophages) can be induced by phorbol 12-myristate 13-acetate (PMA) + ionomycin, interferon gamma (IFN-γ) and granulocyte-macrophage colony stimulating factor (GM-CSF) (Chapoval *et al*, 2001). However, even though the B7-H3 mRNA is constitutively present, there is a tight post-transcriptional regulation, as B7-H3 protein expression is limited and maintained at low levels. It seems that microRNA mechanisms are involved in this regulation, as B7-H3 mRNA and protein expression was shown to be inversely correlated with expression of miRNA-29 and miRNA-187 (Wang *et al*, 2014, 2016). Still, aberrant B7-H3 protein expression has been described in various malignancies such as melanoma, glioma, lung cancer, pancreatic cancer, colon cancer, ovarian cancer, breast cancer and gastric cancer (Janakiram *et al*, 2017). In most cases, increased protein expression of B7-H3 correlates with shorter overall survival of patients, as well as with larger tumor size and more invasive tumor grade and was, therefore, identified as a poor prognosis factor (Ingebrigtsen *et al*, 2014; Mao *et al*, 2015). However, in mouse models for lymphoma and mastocystoma, B7-H3 expression was associated with favorable clinical outcomes (Janakiram *et al*, 2017; Sun *et al*, 2010).

The immunomodulatory role of B7-H3 has been studied intensively in the past few years leading to quite contradictory results since these studies showed both co-stimulatory and co-inhibitory activities of B7-H3 on T cells. Additionally, B7-H3 has been shown to interact with NK cells and inhibit their activity leading to reduced NK-mediated lysis both *in vitro* and *in vivo* (Janakiram *et al*, 2017; Lee *et al*, 2017).

On the other hand, B7-H3 has been shown to have non-immunological roles. It promotes osteoblast differentiation and bone mineralization (Suh *et al*, 2004), but it was also shown to exhibit immune cell-independent roles in the context of cancer progression. It was shown to induce expression of matrix-metalloproteinase (MMP) 9 trough Janus kinase 2 and signal

transducer and activator of transcription 3 (Jak2/Stat3) in CRC cell lines (Liu *et al*, 2015) and also showed positive correlation with MMP-2 (Jiang *et al*, 2016), suggesting pro-migratory and pro-invasive roles for B7-H3. Furthermore, it was demonstrated that B7-H3 down-regulates the expression of E-cadherin and β-catenin, and up-regulates N-cadherin and vimentin in CRC at the same time. This would suggest its involvement in epithelial-to-mesenchymal transition and consequently cancer cell invasion, migration and metastasis formation (Jiang *et al*, 2016). B7-H3 also promotes the Warburg effect by increasing protein levels of Hypoxia-inducible factor 1-alpha (HIF1-α) and key enzymes of glycolytic pathway (lactate dehydrogenase A - LDHA, pyruvate dehydrogenase kinase 1 - PDK1) (Lim *et al*, 2016) indicating functions of B7-H3 that might be independent of its role in shaping the immune system's response. Furthermore, recent data showed nuclear localization of B7-H3 in cancer cells, hinting for cell-intrinsic roles for B7-H3 in the absence of an immune compartment (Ingebrigtsen *et al*, 2012). However, little is known about immune cell-independent roles of B7-H3.

In the group of Prof. Dr. med. Sebastian Zeissig, previous work showed that in genetically induced tumor mouse model, B7-H3 expression is increased within tumor cells compared to tumor-infiltrating immune cells, as well as normal tissue of the same mice (unpublished, Fig. 4). Therefore, in order to analyze potential immune cell-independent roles of B7-H3 in CRC, this thesis aimed to establish a B7-H3 knockout in a mouse colorectal cancer cell line using CRISPR/Cas9 technology (Ran *et al*, 2013). These established cell lines were analyzed on the levels of apoptosis, proliferation and, to some extent, metabolic activity in order to evaluate if there are any cell-intrinsic consequences for tumor cell behavior due to the lack of functional B7-H3 protein, independent of the immune system.
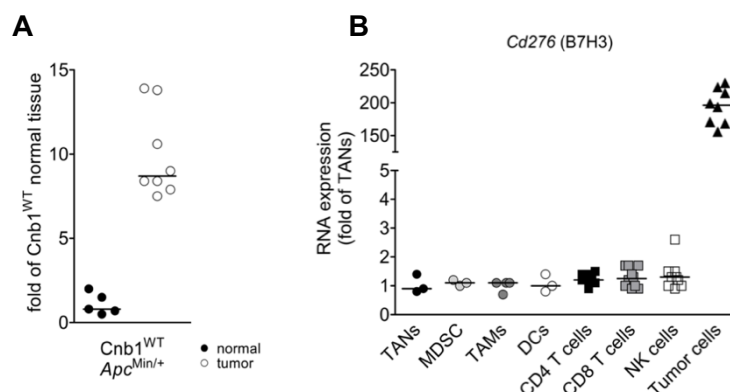
Figure 4. B7-H3 expression is increased in tumor tissue of a genetically induced intestinal tumor mouse model. (**A**) mRNA expression of B7-H3 in normal and tumor tissue of $APC^{Min/+}$ mice shown by qRT-PCR. (**B**) mRNA expression of B7-H3 for distinct cell subsets within intestinal tumor tissue. Each dot represents one mouse. TAN – tumor-associated neutrophils, MDSC – myeloid derived suppressor cells, TAM – tumor-associated macrophages, DC – dendritic cells, NK – natural killer cells (unpublished data, courtesy of Dr. Kenneth Peuker).

2 METHODS

2.1 Molecular methods

2.1.1 Generation of PX458-gB7-H3 plasmid for targeting *Cd276* gene

For targeting the *Cd276* gene (Gene ID: 102657; ncbi.nlm.nih.gov 2017) in murine CMT-93 CRC cells, a pair of DNA oligonucleotides coding for gRNA was designed using the design wizard provided online (Benchling.com, 2017). gRNA targeting exon 3 was chosen depending on its reasonably high on-target score and very good off-target score to minimize off-targeting (Table 1).

Table 1. Oligonucleotide sequences and their on- and off-target scores. Four base pairs (marked in red) had to be added accordingly, in order to ligate the insert into the reading frame of the plasmid.

gRNA		Sequence (5' → 3')	On-target	Off-target
gRNA	(F)	CACCGCGCGTCCGAGTAACCGACGA	71.4	98.8
	(R)	AAACTCGTCGGTTACTCGGACGCGC		

For genome targeting, the mentioned DNA oligonucleotide pair coding for gRNA was cloned into the pSpCas9(BB)-2A-GFP (PX458) plasmid, obtained from Addgene (Addgene plasmid #48138, Appendix A). The plasmid expresses the Cas9 nuclease and gRNA simultaneously, allowing precise gene modifications upon binding of Cas9 to the target sequence. Therefore, PX458 was digested with Fast Digest BpsI (Thermo Fischer Scientific) in 1x FastDigest Buffer (Thermo Scientific) at 37 °C overnight, and later dephosphorylated with Fast AP (Thermo Fisher Scientific) at 37 °C for 10 minutes. Afterwards, the digested plasmid was size fractioned by agarose gel electrophoresis and later purified from the gel using the PureLink Quick Gel Extraction Kit (Invitrogen). Thus, gel slices were dissolved in "Buffer L3" at 50 °C and then loaded onto a DNA-binding column. DNA was bound to the column by centrifugation at 13 000 g for 1 minute. Flow through was discarded and column was washed with "Wash Buffer". "Elution Buffer" was added to the column and incubated for 1 minute at room temperature. Finally, plasmid DNA was collected by centrifugation at 13 000 g for 1 minute. Final concentration was determined using Nanodrop 2000 (Thermo Scientific).

Additionally, the oligonucleotides (Eurofins Genomics) were phosphorylated with T4 PNK (Thermo Fisher Scientific) and annealed using the following protocol: 37 °C for 30 minutes, 95 °C for 5 minutes, ramp down to 25 °C by 0,1 °C/s. The duplexes were ligated into

a linearized PX458 with T4 DNA Ligase (Thermo Fisher Scientific) at 17 °C overnight and afterwards heat-inactivated at 65 °C for 10 minutes.

The ligated plasmids were transformed into chemically competent *Echerichia coli* (*E. coli*) strain Stbl3 (Thermo Fisher Scientific) via heat-shock. Stbl3 were thawed on ice, 5 µl of the ligation mix was added to the bacteria, followed by incubation on ice for 30 minutes, heat-shock (42 °C) for 30 seconds, cooling down on ice for 2 minutes and then incubated in 250 µl LB medium at 37 °C for 1 hour with shaking Finally, bacteria were spread onto Luria-Bertani (LB) plates with ampicillin (Amp+, 100 ng /ml) and incubated overnight at 37 °C.

Next day, single bacterial colonies were picked with sterile pipette tips and transferred into round-bottom tubes in 5 ml of LB Amp+ medium (100 µg /ml), and incubated overnight at 37 °C with shaking. After approximately 18 hours, plasmid DNA was isolated using the Thermo Scientific GeneJET Plasmid Miniprep Kit. Bacterial cultures were harvested by centrifugation at 8000 rpm for 2 minutes. Pellet was resuspended in "Resuspension Solution", cells were lysed by addition of "Lysis Buffer", followed by "Neutralization Buffer" and centrifugation at 12 000 g. Supernatant was transferred to a DNA-binding column and DNA was bound to it by centrifugation at 12 000 g for 1 minute. Column was washed twice with "Wash Solution", and afterwards membrane was dried by centrifugation at 12 000 g for 2 minutes. "Elution Buffer" was added to the membrane and incubated for 2 minutes at room temperature. Plasmids were collected by centrifugation at 12 000 g for 2 minutes. Finally, plasmids were sent for sequencing (GATC Sanger sequencing) (Table 7) and later analyzed by ApE (M. Wayne Davis).

Validated plasmids were again transformed into Stbl3 as described and propagated on a larger scale via Maxiprep (Qiagen EndoFree Plasmid Maxi Kit). Bacterial cultures (250 ml) were harvested by centrifugation at 6000 g for 15 minutes at 4 °C, Pellet was resuspended in "Buffer P1". Cells were lysed by addition of "Buffer P2" and incubation at room temperature for 5 minutes. Lysis was stopped by addition of chilled "Buffer P3". Lysate was filtered and "Buffer ER" was added to the filtrate, which was then incubated on ice for 30 minutes. Filtered lysate was applied to a column, which was later washed twice with "Buffer QC". DNA was eluted with "Buffer QN" and precipitated by addition of isopropanol and centrifugation at 15 000 g for 30 minutes at 4 °C. Pellet was washed with 70% ethanol at 15 000 g for 10 minutes, air dried, redissolved in "Buffer TE" and stored at -20 °C for further use.

2.1.2 Genotyping by polymerase chain reaction (PCR)

Whole cell DNA of CMT-93 cells transfected with control vector or vector containing gRNA-coding sequence (PX458-gB7-H3; vector map in the appendix) was isolated by addition of 50 mM NaOH and boiling for 30 minutes at 100 °C, with a final addition of 10 μl of 1 M Tris/HCl (pH 8). PCR genotyping was done using the primers listed in Table 7 and set up according to Table 2 and Table 3.

Table 2. PCR genotyping reaction mix.

Reagent	μl per reaction	Final concentration
5x OneTaq Buffer (NEBioLabs)	5	1x
dNTP mix (10 mM)	0.5	200 μM
Forward primer	0.1	0.2 μM
Reverse primer	0.1	0.2 μM
OneTaq Polymerase (NEBioLabs)	0.125	1.25 U/50 μl
Nuclease-free water	17.675	NA
DNA	1.5	< 1000 ng
Total volume	**25**	

Table 3. PCR genotyping amplification protocol.

Step	Temperature	Time	
Initial denaturation	94 °C	30 sec	
Denaturation	94 °C	30 sec	
Annealing	56 °C	30 sec	35 cycles
Elongation	68 °C	1 min	
Final elongation	68 °C	5 min	
Hold	4 °C	∞	

PCRs from all clones were first analyzed on a QIAxcel fragment analyzer and the clones which showed a different size than the expected 252 (*Cd276* (B7H3)_1) or 934 base pairs (*Cd276* (B7-H3)_2) were further size fractioned on an agarose gel. Fragments of interest were isolated from the gel using the NucleoSpin Gel and PCR Clean-up kit (Macherey-Nagel). Thus, "Buffer NTI" was added to gel slices and incubated at 50 °C until dissolved. Samples were loaded onato a DNA binding column and centrifuged at 11 000 g for 1 minute. Column was

washed twice with "Buffer NT3", and membrane was dried by centrifugation at 11 000 g for 1 minute. "Elution Buffer" was heated to 70 °C and added to the column which was then incubated for 5 minutes at 70 °C. PCR fragments were collected by centrifugation at 11 000 g for 1 minute. Isolated PCR fragments were sent for sequencing in order to check for potential mutations. Mutations were discovered by alignment of the obtained sequence to the known sequence of *Cd276* using ApE.

2.1.3 cDNA sythesis and real time PCR

Whole cell mRNA was isolated using the PeqGold Total RNA Kit (VWR, peqlab). Culture medium was aspirated completely and "RNA Lysis Buffer T" was added. Cells were scraped to aid cell lysis. Lysate was transferred into a DNA-removing column and centrifuged at 12 000 g for 1 minute at room temperature. Equal volume of 70% ethanol was added to the flow through, which was then transferred into a RNA-binding column. RNA was bound by centrifugation at 10 000 g for 1 minute. Column was washed with "RNA Wash Buffer I" and "RNA Wash Buffer II" and membrane was dried by centrifugation at 10 000 g for 2 minutes. RNA was eluted in RNase free H_2O. cDNA was synthesized using the High-capacity cDNA Reverse Transcription kit (Thermo Fisher Scientific) according to Tables 4 and 5. Real time PCR was performed using SYBR Green (Thermo Fisher Scientific), primers (Table 7) and the appropriate protocol (Table 6) on the real time PCR machine Stratagene MX 3005P. Relative gene expression was calculated from C_t values using the $\Delta\Delta C_t$ method (Livak and Schmittgen, 2001).

Table 4. cDNA synthesis reaction mix

Reagent	µl per reaction
10x RT Buffer	2
25x dNTP mix (100 mM)	0.8
10x Random primers	2
Reverse Transcription (RT) Polymerase	1
RNase inhibitor	1
Nuclease free-water	3.2
RNA	10
Total volume	**20**

Table 5. cDNA synthesis protocol

Step	Temperature	Time
Step 1	25 °C	10 min
Step 2	37 °C	120 min
Step 3	85 °C	5 min
Step 4	4 °C	∞

Table 6. qRT-PCR amplification protocol.

Step	Temperature	Time	
Hot start activation	95 °C	10 min	
Denaturation	95 °C	15 sec	
Annealing	55 °C	30 sec	40 cycles
Extension	72 °C	30 sec	

Table 7. Primer sequences for plasmid sequencing, PCR genotyping and sequencing, and qRT-PCR.

	Gene	Direction	Sequence 5'-3'
sequencing	oligonucleotide insertion site in PX458	(F)	GATACAAGGCTGTTAGAGAG
		(R)	AGGCGGGCCATTTAC
PCR genotyping	*Cd276* (B7-H3)_1	(F)	CTGACAGACACCAAACAGCTG
		(R)	AAAGAGTGGAAGCAGAGGGTAC
	Cd276 (B7-H3)_2	(F)	GCCTTCCATTCCGACATAAACG
		(R)	ATTCTGGACCACCCTAAGCATG
qRT-PCR	*Actb* (β-actin)	(F)	AGATGACCCAGATCATGTTTGAG
		(R)	GTACGACCAGAGGCATACAG
	Cd276 (B7-H3) exons 3-4	(F)	CCTGTTGGTGCAAGGCAATG
		(R)	GTCATGCTGGGCTTCGAGTA
	Cd276 (B7-H3) exons 7-8	(F)	GGCCTCTGAAACCCTCTGAA
		(R)	GACAAACCCATTCGTTGGGG

2.2 Cell Culture

2.2.1 General conditions

For this research mouse colorectal carcinoma cell line CMT-93 was used. These cells have epithelial morphology and grow in clumps as an adherent culture.

If not stated differently, cells were grown in Dulbecco's Modified Eagle Medium (DMEM, Gibco) with 10% fetal bovine serum (FBS, BiochromAG/MerksMillipore), 1% L-glutamine (BiochromAG/MerksMillipore) and 1% penicillin/streptomycin (P/S, BiochromAG/MerksMillipore) at 37 °C with 5% CO_2. Upon splitting or experimental use, cells were incubated with trypsin until detached at 37 °C. The reaction was stopped using pre-warmed medium and cells were further handled as needed. For freezing, cells were trypsinized, centrifuged (1 400 rpm, 4 °C, 5 minutes) and the supernatant was removed. Cells were resuspended in 10% dimethyl sufoxide (DMSO, Sigma Aldrich) in FBS and frozen to -80 °C instantly.

2.2.2 Transfection and single cell sort

$3x10^5$ CMT-93 cells per well were seeded in 6-well plates 24 hours prior to transfection. Cells were transfected using 1 μg of the generated plasmid, or PX458 as a control and appropriate amount of Lipofectamine 2000 (Thermo Fisher Scientific). Six hours post-transfection, cells were washed with 1x Dulbecco's phosphate-buffered saline (D-PBS), new media was added, and cells were grown for an additional 48 hours before the single cell sort.

The transfected CMT-93 cells were trypsinized, washed with 1x D-PBS, centrifuged at 1400 rpm and 4 °C for 5 minutes, and resuspended in FACS buffer (1x D-PBS + 10% FBS). Prior to sorting, 7-aminoactionmycin D (7-AAD, BD Bioscience) viability dye was added to the cells. Cells positive for GFP and negative for 7-AAD were sorted using FACS Aria III (BD Bioscience) into flat bottomed 96-well plates containing DMEM with 20% FBS, 2% P/S, 1% L-glutamine per well and grown until confluency. Afterwards, cells were seeded into bigger wells and medium was changed to regular type when clones reached 12-well plate.

2.3 Biochemical methods

2.3.1 Protein recovery

Cells were lysed with 1x radioimmunoprecipitation assay (RIPA) buffer (50 mM Tris-HCl, pH 7.4, 150 mM NaCl, 5 mM EDTA, 1% Igepal, 0.5% sodium desoxycholat, 0.1% SDS),

incubated by shaking at 4 °C for 1 hour and subsequently centrifuged at 13 000 g for 5 minutes. The supernatant was used for further analysis.

Total protein concentration was determined with Bio-Rad Protein Assay Dye Reagent Concentrate by mixing standards or diluted samples (1:30) with diluted concentrate (1:5). Absorbance was measured at 595 nm on FlexStation 3 microplate reader (Molecular Devices).

2.3.2 Protein deglycosylation

Prior to B7-H3 protein analysis via Western blotting, supernatants were treated with Protein-N-glycosidase F (PNGase F, Roche). First, the amounts of buffers 1 and 2 needed for reaction were calculated according to the formula:

$$y = 28 - x$$

$$V(buffer\ 1) = \ 1/2\ y$$

$$V(buffer\ 2) = \ 1/2\ y$$

where x is the volume of protein extract needed for 40 µg of protein to be used for analysis in Western blot.

For the reaction, protein extracts of each sample were mixed with the respective amount of buffer 1 (50 mM Na_3PO_4, 1% SDS, 1% β-mercaptoethanol, 1x complete proteinase inhibitor, pH 7.8), and the mix was incubated for 5 minutes at 95 °C with shaking. After incubation, each mix was left to cool down partially, buffer 2 (50 mM Na_3PO_4, 1% NP-40, 1x complete proteinase inhibitor, pH 7.5) was added and left to cool down to room temperature. Finally, 2 µl of PNGase was added and samples were shaken at 37 °C overnight. Subsequently, for SDS-PAGE, samples were mixed with 5x Laemmli buffer with DTT (16 µl per 40 µg of protein) and H_2O (4 µl per 40µg of protein), incubated in the thermomixer at 60 °C for 20 minutes and subjected to Western blotting as described in 2.3.3.

2.3.3 Western blot

Prior to sodium dodecyl sulfate-polyacrylamide gel electrophoresis (SDS-PAGE) 20 µg of protein was diluted in total volume of 16 ml 1x RIPA buffer with 4 ml of 5x Laemmli buffer with DTT and cooked for 5 minutes at 95 °C (if not stated differently). Samples were loaded on a SDS-PAGE gel composed of stacking and running gels of relevant concentrations (Table 8). 40 µl aliquots were loaded to the gel, stacked at 80 V until protein ladder started to separate,

and then separated at 110 V until finished. The gel was blotted on the methanol-activated polyvinylidene difluoride (PVDF) membrane (Roth) using Trans-Blot Turbo™ Transfer System (Bio-Rad) and semi-dry blotting program (45 minutes, 1.0 A, 25 V). The blots were blocked in 5% skim milk in TBS-T (50 mM Tris/HCl, pH 7.6; 150 mM NaCl; 1% Tween 50) for 1 hour at room temperature and then incubated overnight at 4 °C in appropriate primary antibodies diluted in 5% skim milk in TBS-T (Table 9).

On the following day, membranes were transferred into corresponding secondary antibodies (Table 9) in 5% skim milk/TBS-T and incubated for 1 hour at room temperature. Finally, membranes were incubated for 5 minutes in 1:1 solution of Clarity™ Western ECL Blotting Substrate (Bio-Rad) and then visualized chemiluminilescently using ImageQuant™ LAS 4000 (GE Healthcare).

Table 8. Formulation of 1 X Running and Stacking gels used for SDS-PAGE.

		Running gel		Stacking gel
		7.5%	12.5%	4%
dH_2O	(ml)	4.5	3.5	2.48
Running Gel Buffer	(ml)	2	2	-
Stacking Gel Buffer	(ml)	-	-	0.9
40% PAA	(ml)	1.5	2.5	0.38
TEMED	(μl)	10	10	4.5
10% APS	(μl)	40	40	12

Table 9. Primary and secondary antibodies used for Western blotting.

	Antibody	Dilution	Source	Company
Primary antibodies	Mouse anti-β-actin	1:2000	rabbit	Sigma Aldrich
	Human anti-B7-H3	1:200	goat	R&D Systems
	Mouse anti-PARP	1:2000	rabbit	Cell Signaling
	Mouse anti-caspase 3	1:2000	rabbit	Cell Signaling
Secondary antibodies	HRP-conjugated anti-rabbit IgG	1:1000	goat	NEBioLabs
	HRP-conjugated anti-goat IgG	1:2000	donkey	Santa Cruz Biotechnology

2.3.4 Immunofluorescence staining

300,000 cells were seeded onto 12 mm round coverslips. On the next day, cells were washed, and then fixated for 30 minutes in cold 4% paraformaldehyde in 1x D-PBS at 4 °C. After fixation, cells were permeabilized first with 0.02% saponin in 1x D-PBS (5 minutes), and then with 0.02% saponin and 0.2% glycin in 1x D-PBS (10 minutes). Subsequently, cells were blocked with 0.02% saponin and 10% FBS in 1x D-PBS for 30 minutes and incubated in a humid chamber with primary goat anti-B7H3 antibody (1:40 in blocking buffer, R&D Systems) at 4 °C overnight. On the following day, cover slips were incubated in the secondary donkey anti-goat antibody conjugated with Alexa Flour® 488 (1:1000 in blocking buffer, Invitrogen) and DAPI (1:1000 in blocking buffer, Sigma Aldrich) for 1 hour at room temperature, mounted on slides with FluorSave (MerckMillipore) and kept at 4 °C in the dark. Images were taken using Zeiss' Axiovert 200M inverted microscope, and analyzed via ImageJ.

2.4 Functional *in vitro* assays

2.4.1 BrDU assay

500 000 cells per well were seeded in a 6-well plate. On the next day, 10 µl of 1 mM BrDU solution (BD Biosciences BrDU Flow kit) per ml of medium was added to each well, and cells were incubated at 37 °C for 45 minutes. After incubation, cells were trypsinized, centrifuged and washed with 1x D-PBS. Between each step cells were washed with 1x "BD Perm/Wash Buffer".

After centrifugation, supernatant was removed, as well as in all the following washing steps. Cells were then resuspended in 100 µl of "BD Cytofix/Cytoperm Buffer", incubated on ice for 30 minutes, and afterwards washed with 1 ml of 1x "BD Perm/Wash Buffer". Next, cells were resuspended in 100 µl of "BD Cytoperm Permeabilization Buffer plus", incubated on ice for 10 minutes and again washed with 1 ml of 1x "BD Perm/Wash Buffer". Cells were re-fixed with 100 µl "BD Cytofix/Cytoperm Buffer" 5 minutes on ice, following with the 1x "BD Perm/Wash Buffer" washing step. Subsequently, cells were resuspended in 100 µl of the DNase working solution (300 µg/ml) and incubated at 37 °C for 1 hour. Cells were incubated with FITC anti-BrDU antibody in 1x "BD Perm/Wash Buffer" for 20 minutes at room temperature in the dark and then with 7-AAD solution for 20 minutes on ice in the dark. Cells were resuspended in staining buffer (1x D-PBS with 1% FBS) and acquired on flow cytometer (BD LSR II) using a low flow rate (<400 events/second). Finally, data was acquired using FlowJo.

2.4.2 Growth assay

7 500 cells per well were seeded in triplicates in a 12-well plate for 8 different time points. Starting from day 2, wells for each condition were collected and counted on 8 consecutive days using the hemocytometer.

2.4.3 MTT assay

1 500 cells per well were seeded in triplicates in a 96-well plate for 7 different time points. For each time point, wells with only culture medium served as a blank. The first reading was acquired 5 hours after cells were seeded to allow adherence. This reading was defined as time point zero and would be subtracted for all subsequent readings in order to normalize the actual number of seeded cells. For each time point, through 7 consecutive days, with a final concentration of 10%, MTT solution (Cell Growth Determination Kit, MTT based, Sigma Aldrich) was aseptically added to each well and incubated for 3 hours. After incubation period, the medium was removed and MTT solvent was added in an amount equal to original culture volume. Fluid was pipetted up and down to dissolve the crystals and absorbance was measured at 570 nm and 690 nm with FlexStation 3 microplate reader. For data analysis, 690 nm readings were subtracted from 570 nm reading well by well. The results were then divided by the average zero time point reading for each well to normalize for starting cell numbers. Finally, absorbance values were displayed as a percentage of day zero.

2.4.4 Cell death analysis

300 000 cells per well were seeded in a 12-well plate. On the next day, cells were treated with 1 μM staurosporine (Sigma Aldrich) or DMSO (1:1000) as a vehicle control and incubated at 37 °C for 2.5 hours. Treated cells were either used for Western blot (PARP, Caspase 3), as previously described, or stained with Annexin V and subsequently analyzed by flow cytometry.

Prior to Annexin V staining, cells were trypsinized, centrifuged, washed and resuspended in Annexin V binding buffer. Cells were stained with Annexin V-APC antibody (Biolegend) and 7-AAD according to manufacturer's instructions and analyzed on flow cytometer (BD LSR II), and finally FlowJo.

2.5 Statistics

For multiple testing one-way analysis of variance (ANOVA), followed by Dunnett's test and two-tailed t-test were performed and mean ± standard error of the mean was plotted.

3 RESULTS

3.1 Generation of B7-H3 knockout clones

The aim of this thesis was to analyze possible cell-autonomous roles of B7-H3 in the mouse colorectal cancer cell line CMT-93. I used the CRISPR/Cas9 technology (Ran *et al*, 2013) to abolish B7-H3 expression in CMT-93 cells. First, CMT-93 cells were transfected with either empty vector or the CRISPR plasmid containing coding sequence of gRNA targeting the B7-H3 gene. The transfected cells were single cell sorted via flow cytometry for green fluorescent protein (GFP) expression of the transfected plasmid, leading to 288 control clones and 480 targeted single cell clones.

Out of all sorted control cells, 10 grew further and were analyzed via PCR as a control for the targeted clones. For targeted cells, initially 53 clones grew further after sorting. However, only 27 clones survived and were screened for mutations in the *Cd276* (B7-H3) gene via PCR.

Out of those 27 clones, a total of 16 clones showed aberrant fragment lengths of the PCR products after size fractionation (Fig. 5). 11 clones showed multiple fragments including the wild type allele, indicating heterozygosity of *Cd276* mutations in these clones. Four clones had fragments which were clearly distinguishable from the wild type clones. However, one clone (4C11) showed no fragments at all, indicating that the introduced mutation might have been considerably different in size than initially expected. Therefore, the PCR was repeated with primers producing a longer (934 bp long) amplicon. In this case, a fragment was detected (Appendix B) indicating that the introduced mutation in this specific clone was a deletion longer than 252 base pairs. All clones which showed a clearly different (potentially homozygous) band pattern compared to the control cells in the PCR were sequenced to analyze the amplified gene sequences and predict a possible loss of protein expression due to frameshift mutations.

From the 5 sequenced clones, all showed a mutation in the targeted region and 3 out of 5 (4D6, 4H12, 6B6) had a mutation predicted to lead to a frameshift and, consequently, a premature stop codon (Tab. 10). For clone 4C11, the protein size could not be predicted as the mRNA splice site was lost due to the deletion.
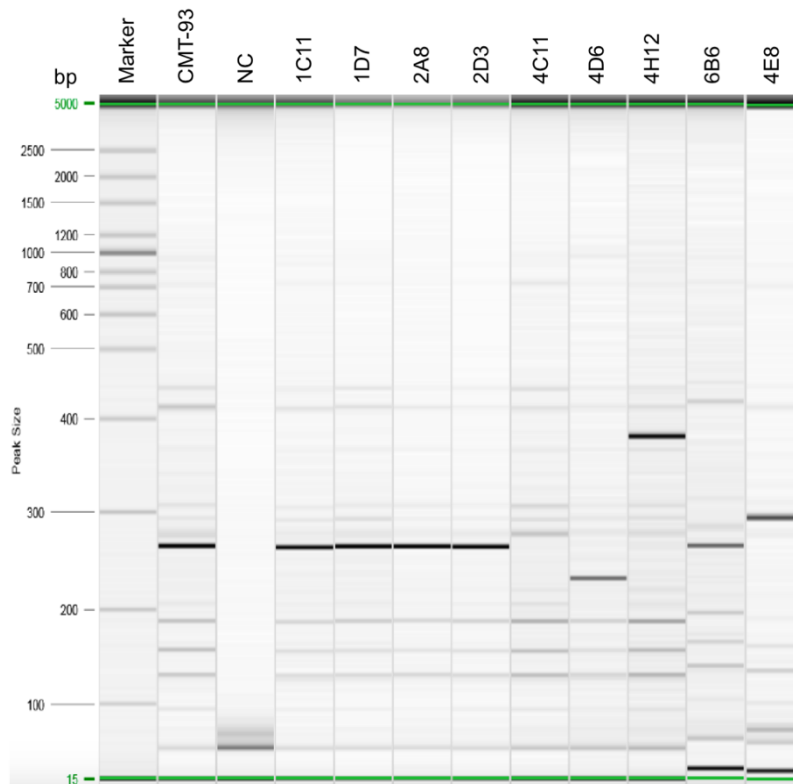
Figure 5. Mutations in the *Cd276* (B7-H3) gene after transfection and single cell sort. PCR of possible mutation sites in single cell sorted CMT-93 cells after transfection with empty vector or vector containing gRNA-coding sequence to target the B7-H3 gene. Untransfected CMT-93 cells were used as a control, and water as a negative control (NC). Clones 1C11, 1D7, 2A8 and 2D3 represent individual empty vector clones whose expected band size (approx. 252 bp) is the same as the untransfected control. Potential knock-out clones are 4C11, 4D6, 4H12, 6B6 and 4E8.

Table 10. Overview of the clones carrying B7-H3 mutations. Length of mutation for each clone and the predicted protein size. Protein size was predicted according to the coding sequences and their respective changes via Benchling.com. All sequences can be found in Appendix C.

Clone name	Mutation	Predicted protein size (AA)
4C11	324 bp deletion	NA
4D6	32 bp deletion	119
4E8	27 bp insertion	325
4H12	109 bp insertion	166
6B6	7 bp deletion	122

3.2 Mutated clones are deficient in B7-H3

After discovering 4 clones with a potential loss-of-function mutation in B7-H3 (4C11, 4D6, 4H12 and 6B6), qRT-PCR and Western blots were performed to confirm that these clones had lost B7-H3 expression. First, mRNA levels were analyzed via qRT-PCRs (Fig. 6A, 6B). To this end, two primer sets were used. One set binds around the mutation site to confirm a possible reduction in the mRNA levels, and the second primer pair binds farther from the mutation site, toward the 3'-end of B7-H3 mRNA in order to ensure that a negative result is not obtained due to a lack of primer binding. As controls, the clones 1C11, 1D7, 2A8, 2D3, which were transfected with an empty vector, were used in all further experiments (Fig. 5).

The mutated clones showed a reduction in B7-H3 mRNA levels regardless of the primer pair used (Fig. 6A, 6B). However, the differences in expression were only significant when primers for the targeted site were used. To confirm these results, B7-H3 expression was analyzed on protein level by Western blot (Fig. 6C). Since B7-H3 is heavily glycosylated, protein samples were treated with protein-N-glycosidase F (PNGase F) to be able to analyze B7-H3 expression as a single band. The Western blot confirmed a band corresponding to B7-H3 at about 40 kDa which was only visible in cell lysates derived from either untransfected or control transfected cells. Hence, the introduced mutations in the *Cd276* gene led to a loss of B7-H3 expression in all 4 mutant clones (Fig. 6C).

In order to further confirm findings from Western blot results, cells were immunofluorescently stained for B7-H3 (Fig. 7). In general, B7-H3 protein is present at moderate levels, and located mostly in the cytoplasm. However, a complete lack of B7-H3 protein was observed in mutant clones with no immunofluorescence signal compared to the control samples (Fig. 7). In conclusion, successful deletion of B7-H3 in the colorectal cancer cell line CMT-93 was achieved via the CRISPR/Cas9 system as documented by qRT-PCR, Western blot and immunofluorescence staining.
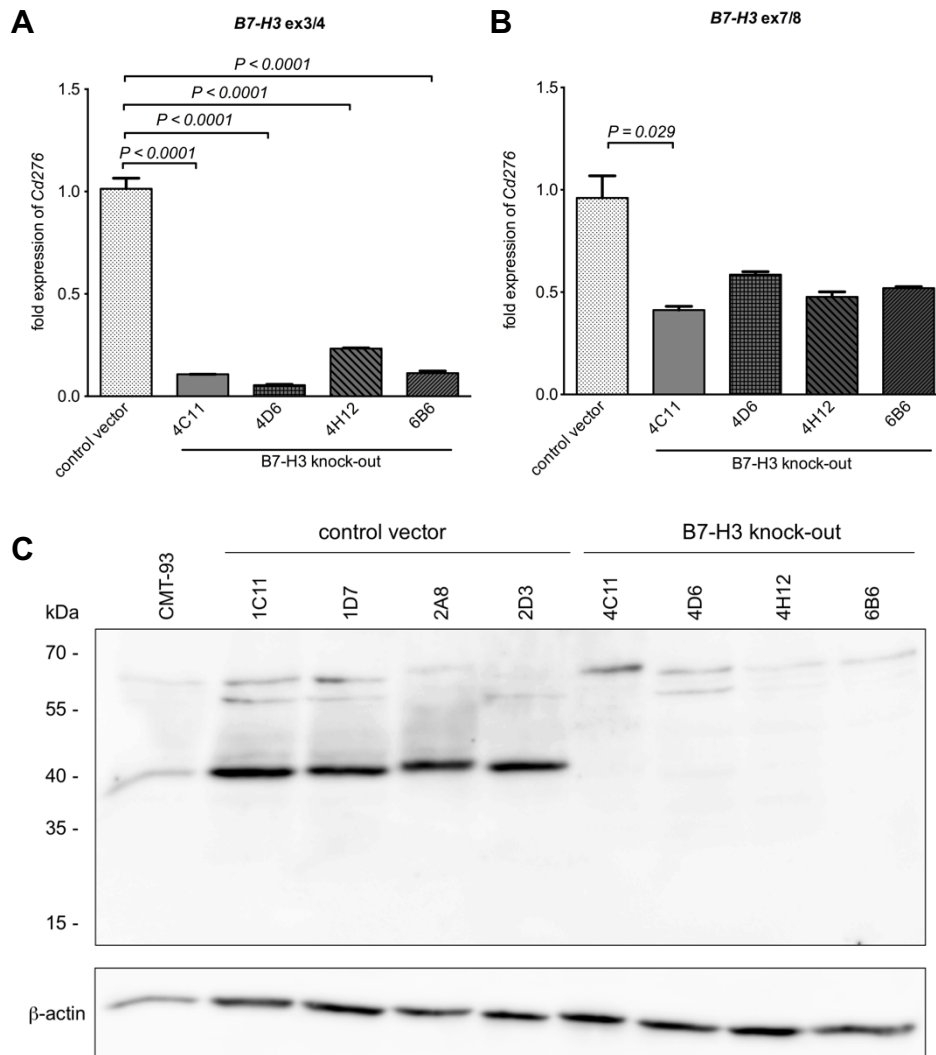
Figure 6. B7-H3 deficiency induced in CMT-93 cells via the CRISPR/Cas9 system. (A-C) Expression of B7-H3 shown by qRT-PCR (A-B) and Western blot (C). qRT-PCR was performed with two different primer pairs either binding around the mutation site (**A**) or at the 3'-end of the mRNA (**B**). As a control, vector transfected clones were used. Multiple testing was done using one-way ANOVA, followed by two-tailed unpaired t-test. (**C**) Representative Western blot from cell lysates derived from CMT-93 cells either untransfected, transfected with control vector or transfected with vector inducing a knockout of B7-H3. Primary antibody: anti-B7-H3, anti-β-actin. All results shown are representative of the two independent experiments.
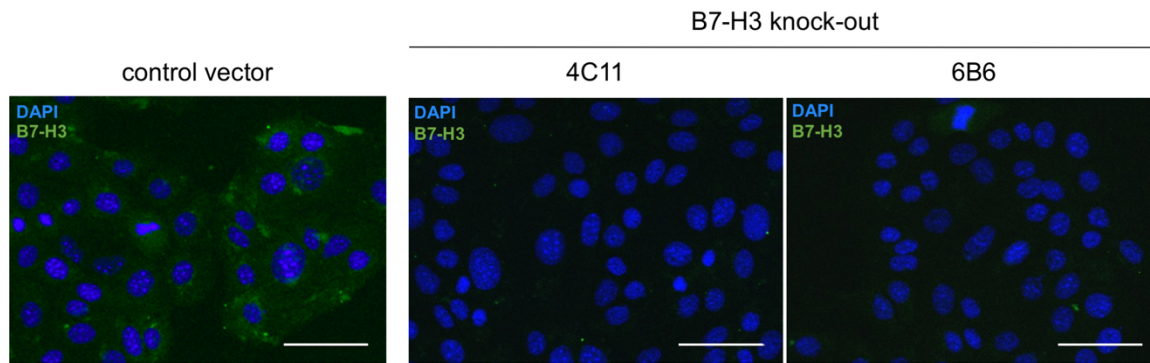
Figure 7. B7-H3 expression is lost in mutant clones. Immunofluorescence staining for B7-H3 (green) in CMT-93 cells transfected either with control vector (left) or a plasmid inducing a knock-out for B7-H3 (middle and right). Representative images are shown. DAPI is shown in blue. Scale bar represents 50 μm.

3.3 Cell death is not altered by B7-H3 deletion

After obtaining clones deficient for B7-H3, we wanted to analyze if there are any cell-autonomous roles for B7-H3 in CRC cells. Therefore, clones deficient for B7-H3 were tested for changes in apoptosis by staining for extracellularly exposed phosphatidylserine using Annexin V and evaluating the levels of cleaved caspase-3 and PARP. As a control, samples were also treated with staurosporine to induce apoptosis.

First, we tested the effect of B7-H3 on apoptosis via Annexin V staining. As seen in Fig. 8A, upon treatment with staurosporine, the percentage of apoptotic cells increased, indicating that the staurosporine treatment was effective. Nevertheless, regardless of the staurosporine treatment, no difference in the percentage of apoptotic cells was noticed between wild-type and B7-H3-deleted clones. Although a strong heterogeneity in apoptosis rates between the different knock-out clones could be detected (Fig. 8A), this heterogeneity did not correlate with residual B7-H3 expression (Fig. 6C).

In addition, the clones were also tested for protein levels of PARP and cleaved caspase-3 as additional markers for apoptosis (Fig. 8B). Caspase-3 was expected at around 33 kDa, while its cleaved form has a size of about 19 kDa. While no cleaved caspase-3 was observed in control settings, the cleaved form of caspase-3 was detected upon staurosporine treatment, indicating that the staurosporine treatment was effective. Nevertheless, similar amounts of cleaved caspase-3 were detected in control compared to B7-H3-deficient cells. On the other hand, PARP Western blots were not successful, and are, therefore, not shown.
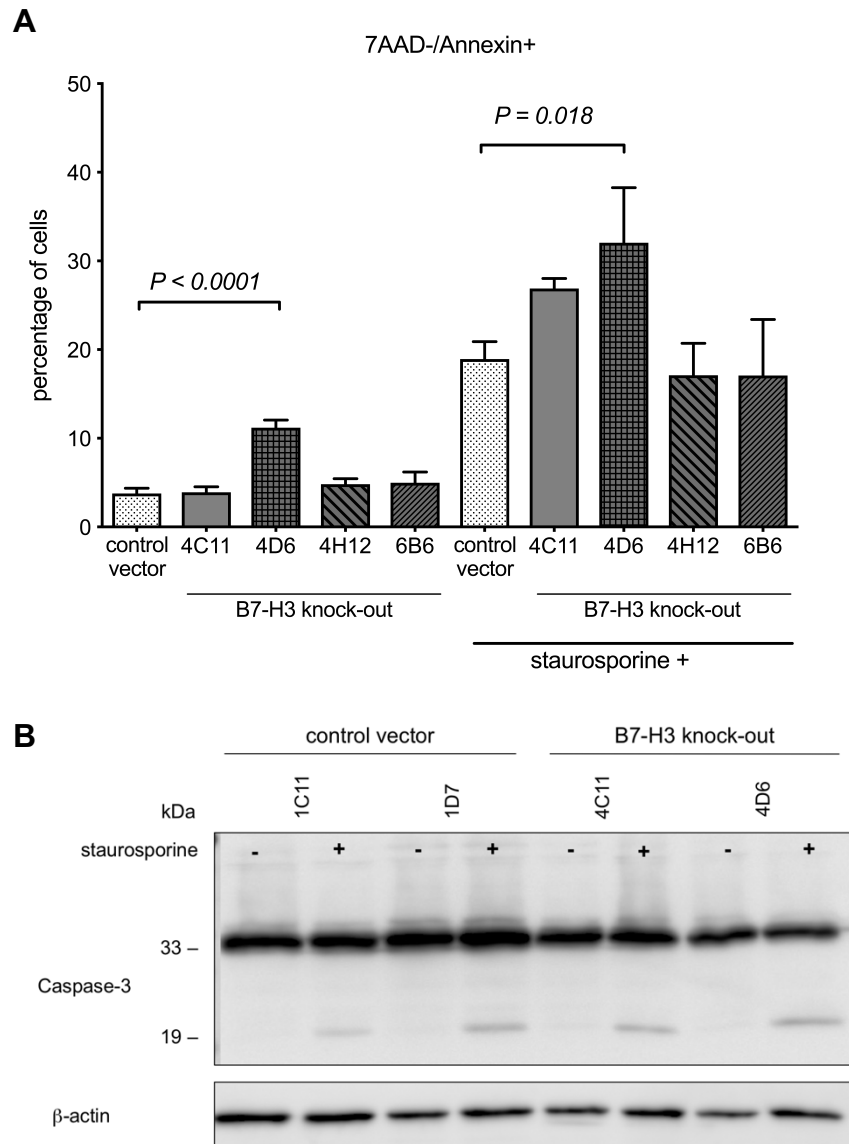
Figure 8. B7-H3 deficiency does not influence apoptosis. (A) Annexin V staining by FACS. Multiple testing was done using one-way ANOVA, followed by two-tailed unpaired t-test. **(B)** Western blot for caspase-3 and β-actin as a loading control. Primary antibodies: anti-caspase 3, anti-β-actin. CMT-93 cells were treated either with vehicle or staurosporine (1 μM) for 2.5 hours **(A-B)**. Vector transfected cells served as negative controls.

3.4 Cell proliferation is not significantly affected by loss of B7-H3 expression

After cell death analysis, I aimed to analyze if B7-H3 influences cellular proliferation in a cell-autonomous manner. To do so, levels of bromodeoxyuridine (BrDU) incorporation, cell growth assays as well as 3-(4,5-dimethylthiazol-2-yl)-2,5-diphenyltetrazolium bromide (MTT) assays were carried out. As seen in Figure 9, no consistent difference in cellular proliferation was noticed in three independent analyses for proliferation between control and

B7-H3-deficient clones. Specifically, no difference between wild-type and knockout clones was found in cell cycle analysis (Fig. 9A). In addition, no significant variation in cell proliferation over time (Fig. 9B) or cell metabolism in terms of mitochondrial activity tested with MTT (Fig. 9C) was found. Although some B7-H3-deficient clones showed slight differences in proliferation rates, these alterations were not consistent among the different knockout clones and among the different experiments carried out, so no role for B7-H3 in the regulation of cell proliferation was observed.
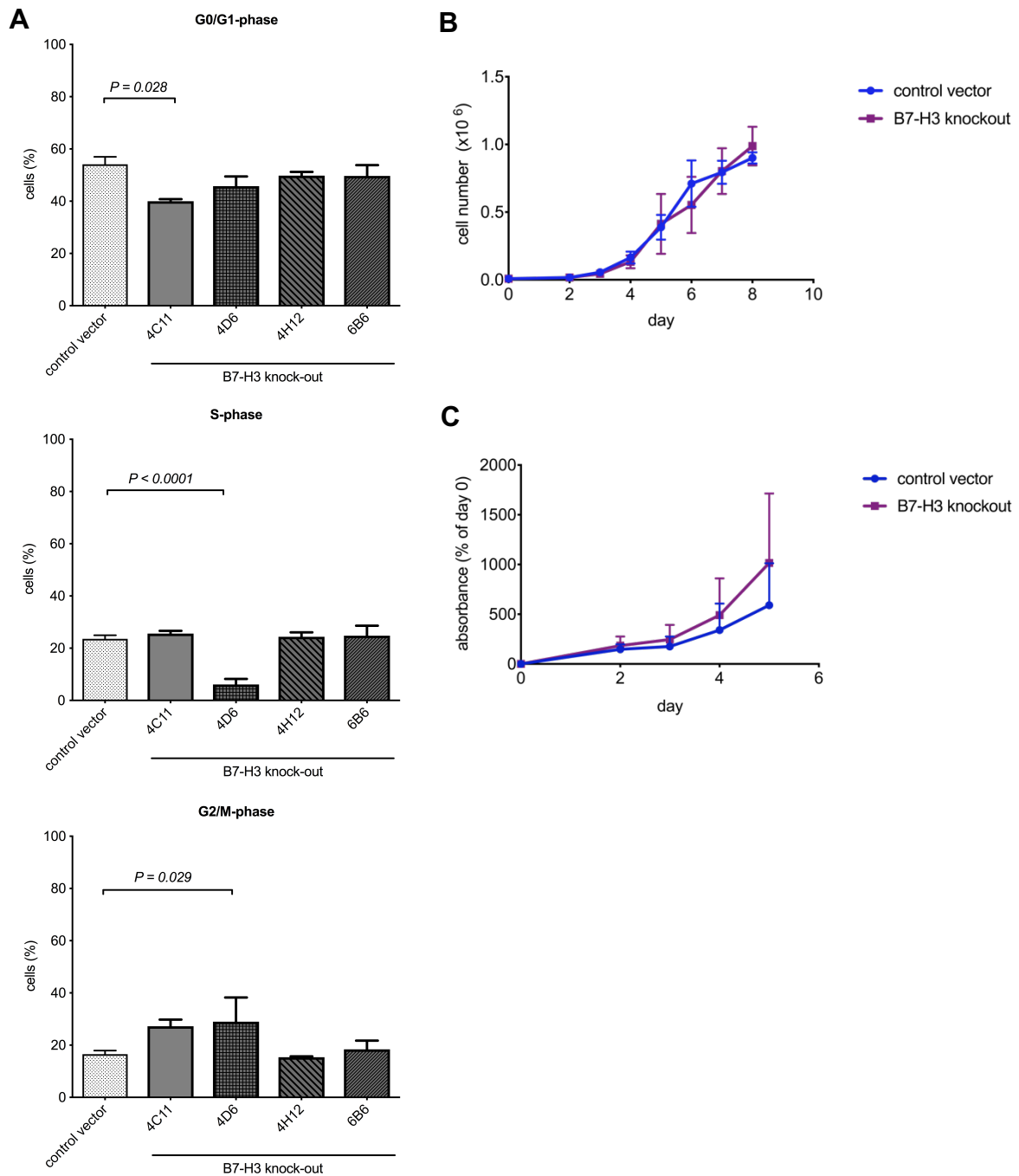
Figure 9. B7-H3 does not regulate cell proliferation. (**A**) Cell cycle analysis of CMT-93 cells as determined using the BrdU assay and FACS. CMT-93 cells, transfected either with control vector or with vector carrying gRNA-coding sequence, were harvested and stained with 10 µM BrdU for 45 minutes. Afterwards, cells were harvested and analyzed via flow cytometry. Vector transfected cells served as negative controls. Multiple testing was done using one-way ANOVA, followed by two-tailed unpaired t-test. Data are mean ± s.e.m. (**B**) Time course for proliferation of CMT-93 cells, transfected either with control vector or with gRNA-containing vector (n = 3 cultures per clone). Data are mean ± SD. (**C**) MTT assay of CMT-93 cells transfected either with control vector or with vector containing gRNA-coding sequence. Data are mean ± SD.

4 DISCUSSION

4.1 Use of CRISPR/Cas9 system to generate B7-H3 knockout clones

The aim of this thesis was to analyze potential cell-autonomous roles of B7-H3 in a CRC cell line. To this end, the CRISPR/Cas9 system was used to generate different knockout clones. I was able to obtain several B7-H3 mutant clones carrying various mutations in B7-H3 that were associated with a frameshift mutation and consequently a premature stop codon. Additionally, clone 4C11 showed a complete loss of the mRNA splice site between exon 3 and 4, which leads to a defect in mRNA splicing. When analyzing the residual expression of B7-H3 in these mutants, they showed reduced levels of B7-H3 mRNA. However, discrepancy in B7-H3 mRNA expression was evident upon testing with two sets of primers. Higher reduction observed using primers amplifying the targeted site could be attributed to the proximity of the mutated site, as the DNA integrity and stability might be disrupted due to the introduced mutations. On the contrary, primers amplifying the 3'-end of the mRNA sequence for B7-H3 showed that the mutant mRNA is still transcribed, although at lower levels, indicating that a small portion of all produced B7-H3 mRNA might be degraded. Nevertheless, since some mRNA of the *Cd276* gene still seemed to be transcribed, it was necessary to analyze B7-H3 protein levels in mutant clones via Western blotting and immunofluorescence staining. Western blot analysis showed only bands at about 40 kDa in the control samples while all mutant clones did not show any expression of B7-H3. This was confirmed by immunofluorescence, which also showed no B7-H3 staining in mutant clones. Taken together, these results imply that all detected mutations lead to a degradation of B7-H3 protein after mRNA translation and that the observed loss of protein is indeed due to premature stop codons or, in case of 4C11, complete change of mRNA composition due to the loss of the mRNA splice site between exons 3 and 4. Therefore, in all mutant clones analyzed, a loss-of-function of B7-H3 was induced.

Via immunofluorescence staining, the intracellular localization of B7-H3 could also be analyzed in CMT-93 cells. In several publications, B7-H3 was shown to be located on the membrane, as well as in the cytoplasm and nucleus (Ingebrigtsen *et al*, 2012, 2014; Janakiram *et al*, 2017). However, my data (Fig. 8) showed no nuclear localization for B7-H3 protein, but rather cytoplasmic localization. Additionally, parallel work by Liz Matthiesen in our lab on CMT-93 cells transiently overexpressing B7-H3 also showed that B7-H3 can be found at the membrane, in the cytoplasm and potentially in lysosomes (data not published). Lack of nuclear localization in CMT-93 cells might be attributed to the fact that nuclear B7-H3 was mainly

reported in human malignancies or *in vivo* CRC models, where B7-H3 could interact with other immune cells (Ingebrigtsen *et al*, 2012, 2014). Furthermore, the cytoplasmic tails of mouse and human B7-H3 have minor differences which might be responsible for different intracellular signaling or localization (Uniprot.org 2017).

4.2   Loss of B7-H3 does not influence apoptosis or proliferation in CMT-93

We set out to analyze the potential role of B7-H3 in regulating cell apoptosis and proliferation in a cell-intrinsic manner. In neither case, we were able to notice any consistent effect of deletion of B7-H3.

In all cases, among wild-type as well as B7-H3 mutant clones, clone-dependent variations in the functional analyses were observed, which was expected due to the fact that mutants were derived from single cells from a heterogeneous CMT-93 population. As we could only see clone-specific differences, but no consistent changes among B7-H3 mutant clones, B7-H3 does not control cell apoptosis and proliferation in CMT-93 cells in a cell-autonomous manner.

Recently, it has also been reported that B7-H3 does not affect apoptosis or proliferation in bladder (T24 and 5637 cells) and hepatic (HepG2 and SMMC7721 cells) carcinoma cell lines (Kang *et al*, 2015; Li *et al*, 2017) in a cell-intrinsic manner, similar to what we have shown in CMT-93 cells. However, in both cases, B7-H3 was knocked-down using an siRNA/shRNA strategy compared to the CRIPSR/Cas9 knock-out strategy used in this study, and thus only exhibit a partial reduction in protein expression. Studies by Kang *et al* (2015) and Li *et al* (2017) thereby showed increased cell migration, invasion and metastasis depending on the expression of B7-H3 in bladder and hepatic carcinoma cell lines. It is therefore important to note that I have so far not addressed whether B7-H3 regulates CRC cell migration and invasion in a cell-autonomous manner. This could be analyzed *in vitro* by scratch wound healing assays or trans-well chamber assays, but also by checking for mRNA and protein expression levels of MMP-2 and -9, E-cadherin, N-cadherin and vimentin. Moreover, since Zhang *et al* (2015) showed that silencing of B7-H3 in HCT-8 cells leads to increased oxaliplatin-induced apoptosis in these cells, it would be interesting to see how mutants would behave in the presence of this specific apoptosis-inducing drug, as it has a different mechanism of action than staurosporine. These additional studies could elucidate if B7-H3 has any cell-autonomous roles in CRC development independent of its potential function in the control of immune cell function.

Furthermore, factors within the tumor microenvironment such as chemokines, cytokines or immune cells could also be introduced in an *in vitro* set up to analyze if the activity of tumor B7-H3 is dependent on the presence of certain parts of the immune system. One example for studying effects within the anti-tumor immune response would be to analyze the ability of B7-H3 mutants to activate OT-I CD8$^+$ T cells. These cells are isolated from transgenic OT-I mice which carry transgenic T cell receptors designed to recognize ovalbumin residues 257-264 in the context of H2Kb, which is a MHC Class I molecule involved in antigen presentation to the T cells. With this, direct interactions between tumor cell-specific B7-H3 and CD8$^+$ T cells and thus non-cell autonomous roles of B7-H3 in the regulation of T cells could be analyzed.

4.3   Prospects

In the future, the generated mutant clones will be used in several different ways. As mentioned, they will be first tested for other potential cell-autonomous roles of B7-H3 such as cell migration, invasion and metastasis, as well as metabolic influences (eg. effects on glucose metabolism). Additionally, effects of B7-H3 on tumor growth and metastatic potential will be further defined in *in vivo* tumorigenicity studies using wild-type C57BL/6 mice and recombination activating gene (*Rag-*)-deficient mice, which lack mature T and B cells. To this end, control and B7-H3 deficient clones will be injected intravenously and subcutaneously into mice which will then be analyzed for tumor formation. In these experiments, cell-autonomous roles as well as T-cell dependent effects can be analyzed in the *Rag1$^{-/-}$* and wild-type background, respectively. Second, immunological roles of B7-H3 in CRC development will be further analyzed by direct investigation of B7-H3-dependent interactions between CRC cells and T cells. As described above, co-cultivation of the CMT-93 knockout clones with OT-I CD8$^+$ T cells will be used to study if B7-H3 acts as a co-stimulatory or co-inhibitory factor in T cell activation, and if it is also involved in the regulation of T cell killing of tumor cells. Finally, and most importantly, we aim to investigate the role of B7-H3 in intestinal tumor development using mice with conditional deletion of B7-H3 within the intestinal epithelium or the immune compartment via the Cre/LoxP system (Le and Sauer, 2000).

5 CONCLUSION

Within this thesis, I was able to generate B7-H3 loss-of-function mutants using CRISPR/Cas9 technology in the mouse CRC cell line CMT-93. I could demonstrate that these mutants do not exhibit cell-intrinsic defects in proliferation and apoptosis as a consequence of loss of B7-H3. The data presented in this thesis suggest that B7-H3 in CRC cells predominantly exhibits non-cell-autonomous roles, e.g. through regulation of antitumor immunity, which will be investigated using tumor models based on intravenous and subcutaneous injection of the generated clones into mice.

6 REFERENCES

Brenner H, Kloor M, Pox CP (2014). Colorectal cancer. *Lancet* **383**: 1490–1502.

Chan DSM, Lau R, Aune D, Vieira R, Greenwood DC, Kampman E, *et al* (2011). Red and processed meat and colorectal cancer incidence: Meta-analysis of prospective studies. *PLoS One* **6**: .

Chaplin DD (2010). Overview of immune response. *J Allergy Clin Immunol* **125**: 41.

Chapoval a I, Ni J, Lau JS, Wilcox R a, Flies DB, Liu D, *et al* (2001). B7-H3: a costimulatory molecule for T cell activation and IFN-gamma production. *Nat Immunol* **2**: 269–274.

Condeelis J, Pollard JW (2006). Macrophages: Obligate partners for tumor cell migration, invasion, and metastasis. *Cell* **124**: 263–266.

Davies RJ, Miller R, Coleman N (2005). Colorectal cancer screening : prospects for molecular stool analysis. *Nat Rev Cancer* **5**: 199-209.

Dunn GP, Old LJ, Schreiber RD (2004). The three es of cancer immunoediting. *Annu Rev Immunol* **22**: 329–360.

Fedirko V, Tramacere I, Bagnardi V, Rota M, Scotti L, Islami F, *et al* (2011). Alcohol drinking and colorectal cancer risk: An overall and dose-Response meta-analysis of published studies. *Ann Oncol* **22**: 1958–1972.

Ferlay J, Soerjomataram I, Dikshit R, Eser S, Mathers C, Rebelo M, *et al* (2015). Cancer incidence and mortality worldwide : Sources , methods and major patterns in GLOBOCAN 2012. **136**: E359-E385.

Formica V, Cereda V, Nardecchia A, Tesauro M, Roselli M (2014). Immune reaction and colorectal cancer: Friends or foes? *World J Gastroenterol* **20**: 12407–12419.

Grivennikov SI, Greten FR, Karin M (2010). Immunity, inflammation, and cancer. *Cell* **140**: 883–899.

Hashiguchi M, Kobori H, Ritprajak P, Kamimura Y, Kozono H, Azuma M (2008). Triggering receptor expressed on myeloid cell-like transcript 2 (TLT-2) is a counter-receptor for B7-H3 and enhances T cell responses. *Proc Natl Acad Sci U S A* **105**: 10495–500.

Ingebrigtsen VA, Boye K, Nesland JM, Nesbakken A, Flatmark K, Fodstad Ø (2014). B7-H3 expression in colorectal cancer: associations with clinicopathological parameters and patient outcome. *BMC Cancer* **14**: 1–9.

Ingebrigtsen VA, Boye K, Tekle C, Nesland JM, Flatmark K, Fodstad O (2012). B7-H3 expression in colorectal cancer: nuclear localization strongly predicts poor outcome in colon cancer. *Int J Cancer* **131**: 2528–2536.

Janakiram M, Shah UA, Liu W, Zhao A, Schoenberg MP, Zang X (2017). The third group of the B7-CD28 immune checkpoint family: HHLA2, TMIGD2, B7x, and B7-H3. *Immunol Rev* **276**: 26–39.

Jess T, Rungoe C, Peyrin-Biroulet L (2012). Risk of colorectal cancer in patients with ulcerative colitis: a meta-analysis of population-based cohort studies. *Clin Gastroenterol Hepatol* **10**: 639–645.

Jiang B, Zhang T, Liu F, Sun Z, Shi H, Hua D, *et al* (2016). The co-stimulatory molecule B7-H3 promotes the epithelial- mesenchymal transition in colorectal cancer. *Oncotarget* **7**: 31755-31771.

Jiang Y, Ben Q, Shen H, Lu W, Zhang Y, Zhu J (2011). Diabetes mellitus and incidence and mortality of colorectal cancer: A systematic review and meta-analysis of cohort studies. *Eur J Epidemiol* **26**: 863–876.

Kang F, Wang L, Jia H, Li D, Li H, Zhang Y, *et al* (2015). B7-H3 promotes aggression and invasion of hepatocellular carcinoma by targeting epithelial-to-mesenchymal transition via JAK2/STAT3/Slug signaling pathway. *Cancer Cell Int* **15**: 1–11.

Le Y, Sauer B (2000). Conditional gene knockout using cre recombinase. *Methods MolBiol* **136**: 477–485.

Lee Y, Martin-Orozco N, Zheng P, Li J, Zhang P, Tan H, *et al* (2017). Inhibition of the B7-H3 immune checkpoint limits tumor growth by enhancing cytotoxic lymphocyte function. *Cell Res* **1**: 1–12.

Lenschow DJ, Walunas TL, Jeffrey A (1996). CD28 / B7 system of T cell costimulation. *Annu Rev Immunol* **14**: 233–58.

Li Y, Guo G, Song J, Cai Z, Yang J, Chen Z, *et al* (2017). B7-H3 promotes the migration and invasion of human bladder cancer cells via the PI3K/Akt/STAT3 Signaling pathway. *J Cancer* **8**: 816–824.

Liang PS, Chen T-Y, Giovannucci E (2009). Cigarette smoking and colorectal cancer incidence and mortality: Systematic review and meta-analysis. *Int J Cancer* **124**: 2406–2415.

Lim S, Liu H, Silva LM Da, Arora R, Liu Z, Phillips JB, *et al* (2016). Immunoregulatory protein B7-H3 reprograms glucose metabolism in cancer cells by ROS-mediated stabilization of HIF1a. *Cancer Res* **76**: 2231–2242.

Liu F, Zhang T, Zou S, Jiang B, Hua D (2015). B7-H3 promotes cell migration and invasion through the Jak2/Stat3/MMP9 signaling pathway in colorectal cancer. *Mol Med Rep* **12**: 5455–5460.

Livak KJ, Schmittgen TD (2001). Analysis of relative gene expression data using real-time quantitative PCR and the $2-\Delta\Delta CT$ method. *Methods* **25**: 402–408.

Lucas C, Barnich N, Nguyen HTT (2017). Microbiota, inflammation and colorectal cancer. *Int J Mol Sci* **18**: 1-27.

Ma Y, Yang Y, Wang F, Zhang P, Shi C, Zou Y, *et al* (2013). Obesity and risk of colorectal cancer: a systematic review of prospective studies. *PLoS One* **8**: e53916.

Mao Y, Li W, Chen K, Xie Y, Liu Q, Yao M, *et al* (2015). B7-H1 and B7-H3 are independent predictors of poor prognosis in patients with non-small cell lung cancer. *Oncotarget* **6**: 3452–3461.

Marcus A, Gowen BG, Thompson TW, Iannello A, Deng W, Wang L, *et al* (2014). Recognition of tumors by the innate immune system and natural killer cells. *Adv immunol* **122**: 91–128.

Ni L, Dong C (2017). New checkpoints in cancer immunotherapy. *Immunol Rev* **276**: 52–65.

Pardoll DM (2012). The blockade of immune checkpoints in cancer immunotherapy. *Nat Rev Cancer* **12**: 252–264.

Pecorino L (2012). Molecular Biology of Cancer: Mechanisms, targets, and therapeutics. *Oxford University Press*, Oxford

Ran F, Hsu P, Wright J, Agarwala V (2013). Genome engineering using the CRISPR-Cas9 system. *Nat Protoc* **8**: 2281–308.

Simone V De, Pallone F, Monteleone G, Stolfi C (2013). Role of TH17 cytokines in the control of colorectal cancer. *Oncoimmunology* **2**: e26617.

Suh W-K, Gajewska BU, Okada H, Gronski M a, Bertram EM, Dawicki W, *et al* (2003). The B7 family member B7-H3 preferentially down-regulates T helper type 1-mediated immune responses. *Nat Immunol* **4**: 899–906.

Suh W-K, Wang SX, Jheon a H, Moreno L, Yoshinaga SK, Ganss B, *et al* (2004). The immune regulatory protein B7-H3 promotes osteoblast differentiation and bone mineralization. *Proc Natl Acad Sci U S A* **101**: 12969–12973.

Sun J, Chen LJ, Zhang GB, Jiang JT, Zhu M, Tan Y, *et al* (2010). Clinical significance and regulation of the costimulatory molecule B7-H3 in human colorectal carcinoma. *Cancer Immunol Immunother* **59**: 1163–1171.

Sun J, Fu F, Gu W, Yan R, Zhang G, Shen Z, *et al* (2011). Origination of new immunological functions in the costimulatory molecule B7-H3: The role of exon duplication in evolution of the immune system. *PLoS One* **6**: e25751.

Taylor D, Burt R, Williams M, Haug P, Cannon-Albright L (2010). Population-based family-history-specific risks for colorectal cancer: a constellation approach. *Gastroenterology* **138**: 877–885.

Terzic J, Karin E, Karin M (2010). Inflammation and Colon Cancer. *Gastroenterology* **138**: 2101–2114.

Tosolini M, Kirilovsky A, Mlecnik B, Fredriksen T, Mauger S, Bindea G, *et al* (2011). Clinical impact of different classes of infiltrating T cytotoxic and helper cells (Th1, Th2, Treg, Th17) in patients with colorectal cancer. *Cancer Res* **71**: 1263–1271.

Wang L, Kang FB, Shan BE (2014). B7-H3-mediated tumor immunology: Friend or foe? *Int J Cancer* **134**: 2764–2771.

Wang Z-S, Zhong M, Bian Y-H, Mu Y-F, Qin S-L, Yu M-H, *et al* (2016). MicroRNA-187 inhibits tumor growth and invasion by directly targeting CD276 in colorectal cancer. *Oncotarget* **7**: 44266–44276.

Zhang T, Jiang B, Zou ST, Liu F, Hua D (2015). Overexpression of B7-H3 augments anti-apoptosis of colorectal cancer cells by Jak2-STAT3. *World J Gastroenterol* **21**: 1804–1813.

INTERNET REFERENCES

www.benchling.com (Jan 2017)

www.globocan.iarc.fr (Aug 2017)

www.hopkinscoloncancercenter.org (Aug 2017)

www.ncbi.nlm.nih.gov/gene/102657 (Jan 2017)

www.uniprot.org/uniprot/Q5ZPR3 (Oct 2017)

www.uniprot.org/uniprot/Q8VE98

7   APPENDICES

1. APPENDIX A: Vector map for PX458
2. APPENDIX B: Possible off-target sites for gRNA
3. APPENDIX C: Gel image for 934bp long PCR amplicon
4. APPENDIX D: Sequences and alignments of mutant clones
5. APPENDIX E: Composition of buffers

PX458 (gB7-H3)
9292 bp
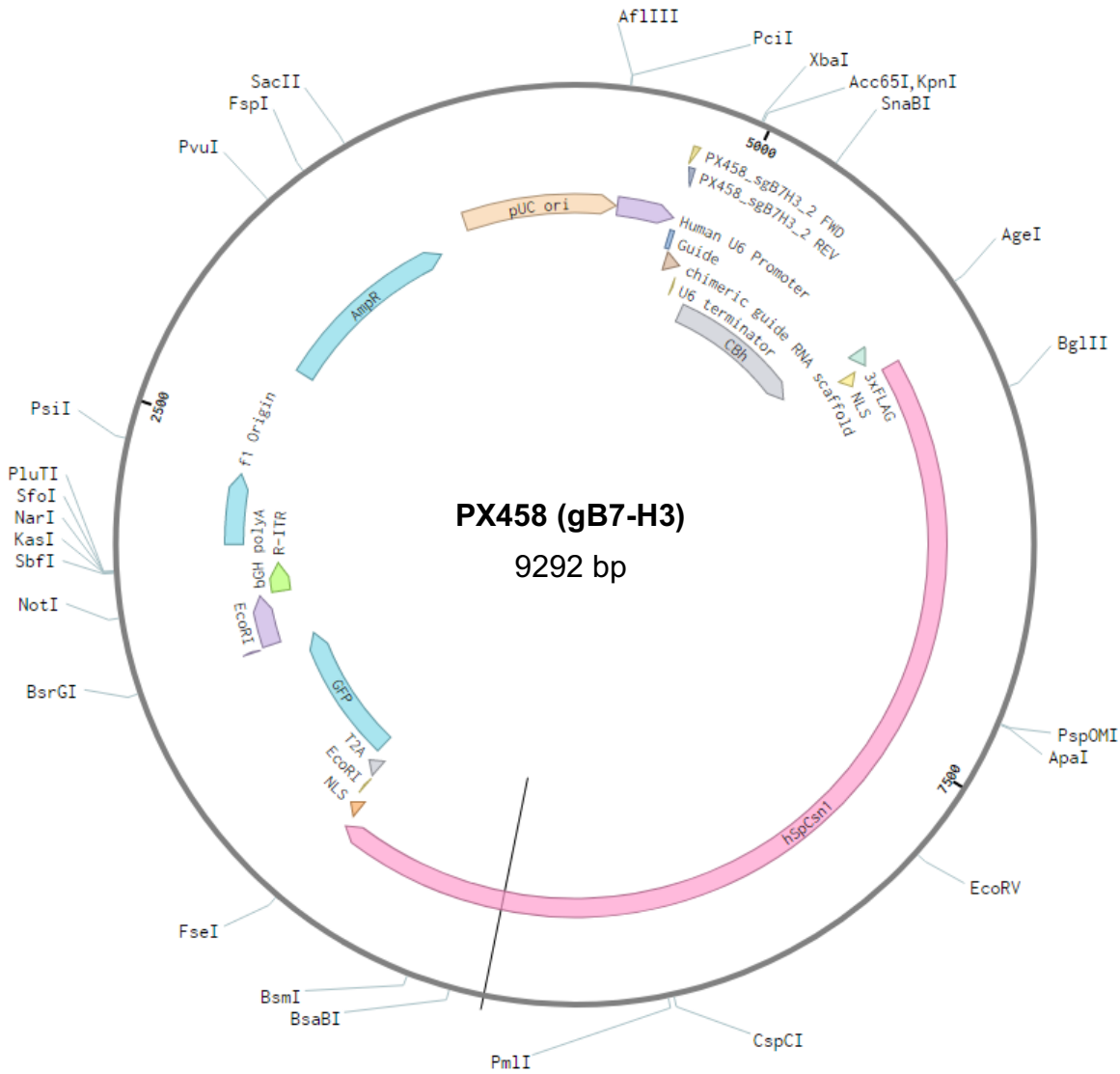
APPENDIX B: Possible off-target sites for gRNA

Targeted sequence	Gene	Chromosome	Position
AGAGTCCTAGGAACCGACGA	NA	chr11	51085046
CGCCTCCGAGCAGCCGCCGA	Fam115a	chr6	42693036
AGCGTCCGAGAACCTGACGA	NA	chr17	28042566
CGCGGCCGAGGAACCAACAA	NA	chr16	28929235

APPENDIX C: Gel image for 934bp long PCR amplicon
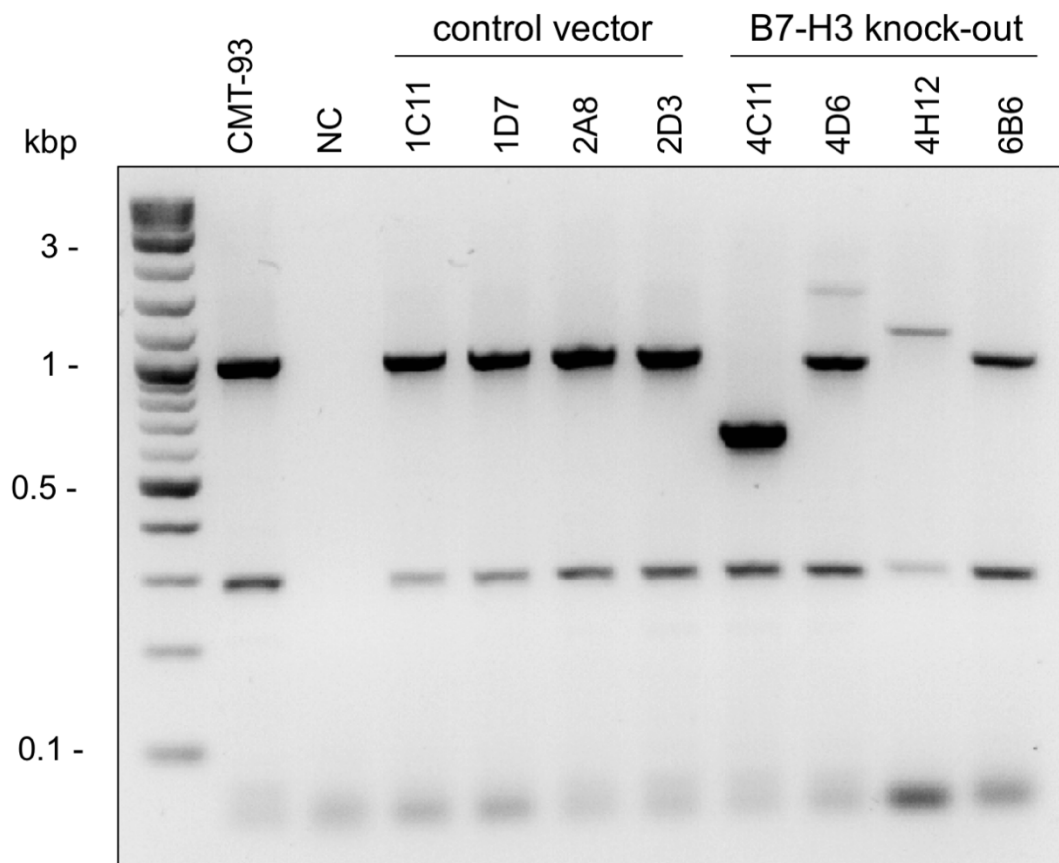
APPENDIX D: Sequences and alignments of mutant clones in the targeted part. Top sequence is the *Cd276* reference sequence, and other two sequences were obtained by sequencing using forward and reverse primers respectively. Inserted or deleted parts are marked in red.

4D6

```
            *         *         *         *         *         *         *         *         *         *
  1>CTGACAGACACCAAACAGCTGGTGCACAGCTTCACGGAGGGCCGGGACCAAGGCAGTGCCTACTCCAACCGCACAGCGCTCTTCCCTGACCTGTTGGTGC>100
  1>~~~~~~~~~~~~~~~~~~~~~~~~~~NNNNNNCGNAGG--CGGGNC--AGGCAGTGCCTACTCCAACCGCACAGCGCTCTTCCCTGACCTGTTGGTGC>68
194<CTGACAGACACCAAACAGCTGGTGCACAGCTTCACGGAGGGCCGGGACCAAGGCAGTGCCTACTCCAACCGCACAGCGCTCTTCCCTGACCTGTTGGTGC<95

            *         *         *         *         *         *         *         *         *         *
101>AAGGCAATGCGTCCTTGAGGCTGCAGCGCGTCCGAGTAACCGACGAGGGCAGCTACACCTGCTTTGTGAGCATCCA-GGACTTTGACAGCGCTGCTGTTA>199
 69>AAGGCAATGCGTCCT-------------------------------------GGCAGCTACACCTGCTTTGTGAGCATCCA-GGACTTTGACAGCGCTGCTGTTA>135
 94<AAGGCAATGCGTCCT-------------------------------------GGCAGCTACACCTGCTTTGTGAGCATCCAGGGACTTTGACAGCGCTGCTGTTA<27

            *         *         *         *         *         *
200>GCCTGCAGGTGGCCGG-TGAGCGTGGAGAGGGGTACCCTCTGCTTCCACTCTTT~>252
136>GCCTGCAGGTGGCCGG-TGAGCGTGGAGAGGGGTACCCTCTGCTTCCACTCTTTA>189
 26<GCCTGCAG-T-GCCGGATGA-C-T-GAGCGG~~~~~~~~~~~~~~~~~~~~~~~<1
```

4C11

```
            *         *         *         *         *         *         *         *         *         *
399>GAGGGCCGGGACCAAGGCAGTGCCTACTCCAACCGCACAGCGCTCTTCCCTGACCTGTTGGTGCAAGGCAATGCGTCCTTGAGGCTGCAGCGCGTCCGAG>498
369>GAGGGCCGGGACCAAGGCAGTGCCTACTCCAACCGCACAGCGCTCTTCCCTGACCTGTTGGTGCAAGGCAATGCGTCCTTGAGGCTGCAGCGCGTCCG-->466
184<GAGGGCCGGGACCAAGGCAGTGCCTACTCCAACCGCACAGCGCTCTTCCCTGACCTGTTGGTGCAAGGCAATGCGTCCTTGAGGCTGCAGCGCGTCCG--<87

            *         *         *         *         *         *         *         *         *         *
499>TAACCGACGAGGGCAGCTACACCTGCTTTGTGAGCATCCAGGACTTTGACAGCGCTGCTGTTAGCCTGCAGGTGGCCGGTGAGCGTGGAGAGGGGTACCC>598
466>------------------------------------------------------------------------------------------------->466
 87<-------------------------------------------------------------------------------------------------<87

            *         *         *         *         *         *         *         *         *         *
599>TCTGCTTCCACTCTTTATCCTTCTGCATGTGGCCTCTCACACGCTGCTGTACCACAGATGAGCCTGCGCTAACAGCCTGTGCGCCTTCCACTATCTCCTG>698
466>------------------------------------------------------------------------------------------------->466
 87<-------------------------------------------------------------------------------------------------<87

            *         *         *         *         *         *         *         *         *         *
699>CACTGATGCTGTTGGTGATGATCCCTGTCCTCTGCCACCTTCCAGCCTTCTACTCAAAGCCCAGCATGACTCGGGAGCCCAACAACCTGGGGACAAGGTG>798
466>------------------------------------------------------------------------------------------------->466
 87<-------------------------------------------------------------------------------------------------<87

            *         *         *         *         *         *         *         *         *
799>ACATCATATGTACCAGCTCCCGGGGCTGCCCAGAGGCTGCGGCAGGGCTCAGCAGCCTGGCCTTGTGACGGAATCTTAGGTGGCCAAGGAGCAAGG-CTT>897
467>-----------------------GGGCTGCCCAGAGGCTGCGGCAGGGCTCAGCAGCCTGGCCTTGTGACGGAATCTTAGGTGGCCAAGGAGCAAGG-CTT>543
 86<-----------------------GGGCTGCCCAGAGGCTGCGGCAGGGCTCAGCAGCCTGGCCTTGTGACGGAATCTTAGGTGGCCAAGGAGCAAGGGCTT<9
```

4H12

```
            *         *         *         *         *         *         *         *         *         *
  1>~CTGACAGACACCAAACAGCTGGTGCACAGCTTCACGGAGGGCCGGGACCAAGGCAGTGCCTACTCCAACCGCACAGCGCTCTTCCCTGACCTGTTGGTG>99
  1>~~~~~~~~~~~~~~~~~~~~~~~~~NNNNNTNNNNNNAGG--CGGGA-CAAGGCAGTGCCTACTCCAACCGCACAGCGCTCTTCCCTGACCTGTTGGTG>71
334<TCTGACAGACACCAAACAGCTGGTGCACAGCTTCACGGAGGGCCGGGACCAAGGCAGTGCCTACTCCAACCGCACAGCGCTCTTCCCTGACCTGTTGGTG<235

            *         *         *         *         *         *         *
100>CAAGGCAATGCGTCCTTGAGGCTGCAGCGCGTCCGAGTAACCGAC---------------------------------------------------->144
 72>CAAGGCAATGCGTCCTTGAGGCTGCAGCGCGTCCGAGTAACCGACAAGGTCGCCCGACGCCCGGGCTTTGCCCGGGCGGCCTCAGTGAGCGAGCGAGCGC>171
234<CAAGGCAATGCGTCCTTGAGGCTGCAGCGCGTCCGAGTAACCGACAAGGTCGCCCGACGCCCGGGCTTTGCCCGGGCGGCCTCAGTGAGCGAGCGAGCGC<135

            *         *         *         *         *         *
145>-----------------------------------------------------GAGGGCAGCTACACCTGCTTTGTGAGCATCCAGGACTTTGACAGCG>190
172>GCAGAGAGGGAGTGGCCAACTCCATCACTAGGGGTTCCTGCGGCCGCTCCCCACGAGGGCAGCTACACCTGCTTTGTGAGCATCCAGGACTTTGACAGCG>271
134<GCAGAGAGGGAGTGGCCAACTCCATCACTAGGGGTTCCTGCGGCCGCTCCCCACGAGGGCAGCTACACCTGCTTTGTGAGCATCCAGGACTTTGACAGC<35

            *         *         *         *         *         *         *         *
191>CTGCTGTTAGCCTGCAGGTGGCCGGTGAGCGTGGAGAGGGGTACCCTCTGCTTCCACTCT-TT~~~~~~~~~>252
272>CTGCTGTTAGCCTGCAGGTGGCCGGTGAGCGTGGAGAGGGGTACCCTCTGCTTCCACTCT-TTAAAANNNNG>342
 34<CTGCTGTTAGCCTGCAG-TG-------------------------CCTCT--ATC-A-TCTAGA~~~~~~~~~<1
```

6B6

```
                  *         *         *         *         *         *         *         *         *         *         *         *         *
    1>~~~~~~~~~~~~~~~~~~~~~~~~~~~~~~~~~~~~~~~~~~~~~~~~~~~~~~~~~~~~~~~~~~~~~~~~~CTGACAGACACCAAACAGCTGGTGCACAGCTT>32
    1>~~~~~~~~~~~~~~~~~~~~~~~~~~~~~~~~~~~~~~~~~~~~~~~~~~~~~~~~~~~~~~~~~~~~~~~NNNTNNNNNNNNAAA------------------->15
  287<AAAGAGTGGAAGCAGATAAAAGCATGGAAGCTGAGGCTACCTAAATGGACTCTGACAGCTAAAGACATCTGACAGACACCAAACAATTGGGGCACAGCTT<188

                  *         *         *         *         *         *         *         *         *         *         *         *         *
   33>CACGGAGGGCCGGGACCAAGGCAGTGCCTACTCCAACCGCACAGCGCTCTTCCCTGACCTGTTGGTGCAAGGCAATGCGTCCTTGAGGCTGCAGCGCGTC>132
   16>---GGA----CGGNAC--AGGCAGTGCCTACTCC-ACCGCACAGCGCTCTTCCCTGACCTGTTGGTGCAAGGCAATGCGTCCTTGAGGCTGCATCGCGTC>105
  187<CACGGAGGTCCGGGACCAAGGCAGTGCCTACTACAACCGCACAGCGCTCTTCCTTGACTTGTTGGTGCAAGGCAATGTGTCCTTGAGGCTGCAGCGTGTC<88

                  *         *         *         *         *         *         *         *         *         *         *         *         *
  133>CGAGTAACCGACGAGGGCAGCTACACCTGCTTTGTGAGCATCCAGGACTTTGACAGCGCTGCTGTTAGCCTGCAGGTGGCCGGTGAGCGTGGAGAGGGGT>232
  106>CGAGTA-------AGGGCAGCTACACCTGCTTTGTGAGCATCCAGGACTTTGACAGCGCTGCTGTTAGCCTGCAGGTGGTCGGCGAGCGTGGAGAGGGGT>198
   87<CGAGTA-------AGGGCAGGTACACCTGCTTTGTGAGCATCCAGGACTTTGTCAGCGAT-ATTATAGCCTGCAGTTGACC--T----------------T<13

                  *         *         *         *         *         *         *         *         *
  233>ACCCTCTGCTTC-CACTCTTT~~~~~~~~~~~~~~~~~~~~~~~~~~~~~~~~~~~~~~~~~~~~~~~~~~~~~~~~~~~~~>252
  199>ACCCTCTGCTTC-CACTCTTTACCCTGCGTCTTCTCTTTATAAATATACGTCCTGTNTAGGTNTNGNTGGCCNTTTCTTT>277
   12<A-------TTCGCAC-GTGG~~~~~~~~~~~~~~~~~~~~~~~~~~~~~~~~~~~~~~~~~~~~~~~~~~~~~~~~~~~~~~~<1
```

IV

APPENDIX E: Composition of Buffers

Kit/Purpose	Buffer	Composition
PureLink Quick Gel Extraction Kit	"Gel Solubilization Buffer L3"	contains guanidinium thiocyanite
	"Wash Buffer"	contains 75-80% ethanol
	"Elution Buffer	10 mM Tris/HCl, pH 8.5
GeneJET Plasmid Miniprep kit	"Resuspension Solution"	contains 10 mg/ml RNase A
	"Lysis Buffer"	contains sodium hydroxide and sodium lauryl sulfate
	"Neutralization Buffer"	contains guanidinium chloride
	"Wash Buffer"	contains 75-80% ethanol
	"Elution Buffer"	10 mM Tris/HCl, pH 8.5
EndoFree Plasmid Maxi Kit	"Buffer P1" (resuspension solution)	50 mM Tris-Cl, pH 8.0
		10 mM EDTA
		100 µg/ml RNase A
	"Buffer P2" (lysis buffer)	200 mM NaOH
		1% SDS (w/v)
	"Buffer P3" (neutralization buffer)	3.0 M potassium acetate
		pH 5.5
	"Buffer ER"	NA
	"Buffer QBT" (equilibration buffer)	750 mM NaCl
		50 mM MOPS, pH 7.0
		15% isopropanol (v/v)
		0.15% Triton X-100 (v/v)
	"Buffer QC" (wash buffer)	1.0 M NaCl
		50 mM MOPS, pH 7.0
		15% isopropanol (v/v)
	"Buffer QN" (elution buffer)	1.6 M NaCl
		50 mM MOPS, pH 7.0
		15% isopropanol (v/v)
	"Buffer TE"	10 mM Tris-Cl, pH 8.0
		1 mM EDTA
NucleoSpin Gel and PCR Clean-up kit	"Buffer NTI"	contains guanidinium thiocyanite
	"Buffer NT3"	contains 75-80% ethanol
	"Elution Buffer NE"	5 mM Tris/HCl, pH 8.5
PeqGold Total RNA Kit	"RNA Lysis Buffer T"	contains guanidinium thiocyanate 40-50%

	"RNA Wash Buffer I"	contains ethanol 25-50%, guanidinium thiocyanate 10-25%
	"RNA Wash Buffer II"	NA
BrDU FlowKit	"BD Cytofix/Cytoperm Buffer"	contains 4.2% formaldehyde
	"BD Cytoperm Permeabilization Buffer Plus"	NA
	"BD Perm/Wash Buffer"	NA
Restriction Digestion	FastDigest Buffer	NA
cDNA synthesis	10x RT Buffer	NA
PCR	5x OneTaq Buffer	NA
Deglycosylation	PNGase Buffer 1	50 mM Na_3PO_4 1% SDS (w/v) 1% b-mercaptoethanol (v/v) 1x complete proteinase inhibitor pH 7.8
	PNGase Buffer 2	50 mM Na_3PO_4 1% NP-40 (v/v) 1x complete proteinase inhibitor pH 7.5
Protein recovery	RIPA Buffer	50 mM Tris/HCl, pH 7.4 150 mM NaCl 5 mM EDTA 1% Igepal (v/v) 0.5% sodium deoxycholat (w/v) 0.1% SDS (w/v)
Western blot	5x Laemmli with DTT	5% SDS (w/v) 50% glycerol (w/v) 625 mM Tris 500 mM DTT
	Running Gel Buffer	1.5 M Tris Base 0.4% SDS (w/v) pH 8.8
	Stacking Gel Buffer	0.5 M Tris Base 0.4% SDS (w/v) pH 6.8

	10x SDS Running Buffer	190 mM glycin
		25 mM Tris
		0.1% SDS (w/v)
	Semi-dry Transfer Buffer	19 mM Tris Base
		0.4% glycin (w/v)
		10% methanol (v/v)
	TBS-T	50 mM Tris/HCl, pH 7.6
		150 mM NaCl
		1% Tween 50 (v/v)
Flow cytometry	FACS Buffer	1x D-PBS
		10% FBS (v/v)
Annexin V staining	Annexin V Binding Buffer	50 mM HEPES
		700 mM NaCl
		12.5 mM $CaCl_2$
		pH 7.4

CURRICULUM VITAE

I was born on July 26th, 1994, in Rijeka. I completed my high school education in my hometown Delnice. In 2012 I enrolled in the Undergraduate programme of Molecular biology at the Faculty of Science, University of Zagreb. I completed laboratory practice under supervision of Assoc. Prof. Dr. Vesna Benković at the Divison of Animal Physiology. During my final year of undergradute studies I was part of the 9th International Society for Applied Biosciences (ISABS) Conference on Forensic and Anthropologic Genetics and Mayo Clinic Lectures in Individualized Medicine. I graduated from the undergraduate programme by writing a final paper titled «Host-microbiome interactions as a driver of evolution and development" under supervision of Dr. Damjan Franjević, Ass. Prof. and obtained a title of bacc.mol.biol.

In September of 2015, I enrolled in the Graduate programme of Molecular Biology. I was a teaching assistant in laboratory practice for Animal Physiology course led by Dr. Benković, Assoc. Prof. Dr. Domagoj Đikić and Prof. Dr. Nada Oršolić. I completed my final year of gradute studies at DFG-Center for Regenerative Therapies Dresden, Cluster of Excellence, TU Dresden within the Erasmus+ student exchange programme. During this time, I also worked on my Master's thesis in the laboratory of Prof. Dr. med. Sebastian Zeissig in the field of mucosal and tumor immunology, under supervision of Prof. Zeissig and Dr. Kenneth Peuker.